

Statistics on the Heterotic Landscape: Gauge Groups and Cosmological Constants of Four-Dimensional Heterotic Strings

Keith R. Dienes*

Department of Physics, University of Arizona, Tucson, AZ 85721 USA

Abstract

Recent developments in string theory have reinforced the notion that the space of stable supersymmetric and non-supersymmetric string vacua fills out a “landscape” whose features are largely unknown. It is then hoped that progress in extracting phenomenological predictions from string theory — such as correlations between gauge groups, matter representations, potential values of the cosmological constant, and so forth — can be achieved through statistical studies of these vacua. To date, most of the efforts in these directions have focused on Type I vacua. In this note, we present the first results of a statistical study of the *heterotic* landscape, focusing on more than 10^5 explicit non-supersymmetric tachyon-free heterotic string vacua and their associated gauge groups and one-loop cosmological constants. Although this study has several important limitations, we find a number of intriguing features which may be relevant for the heterotic landscape as a whole. These features include different probabilities and correlations for different possible gauge groups as functions of the number of orbifold twists. We also find a vast degeneracy amongst non-supersymmetric string models, leading to a severe reduction in the number of realizable values of the cosmological constant as compared with naive expectations. Finally, we also find strong correlations between cosmological constants and gauge groups which suggest that heterotic string models with extremely small cosmological constants are overwhelmingly more likely to exhibit the Standard-Model gauge group at the string scale than any of its grand-unified extensions. In all cases, heterotic worldsheet symmetries such as modular invariance provide important constraints that do not appear in corresponding studies of Type I vacua.

*E-mail address: dienes@physics.arizona.edu

1 Introduction

One of the most serious problems faced by practitioners of string phenomenology is the multitude of possible, self-consistent string vacua. That there exist large numbers of potential string solutions has been known since the earliest days of string theory; these result from the large numbers of possible ways in which one may choose an appropriate compactification manifold (or orbifold), an appropriate set of background fields and fluxes, and appropriate expectation values for the plethora of additional moduli to which string theories generically give rise. Although historically these string solutions were not completely stabilized, it was tacitly anticipated for many years that some unknown vacuum stabilization mechanism would ultimately lead to a unique vacuum state. Unfortunately, recent developments suggest that there continue to exist huge numbers of self-consistent string solutions (*i.e.*, string “models” or “vacua”) even after stabilization. Thus, a picture emerges in which there exist huge numbers of possible string vacua, all potentially stable (or sufficiently metastable), with apparently no dynamical principle to select amongst them. Indeed, each of these potential vacua can be viewed as sitting at the local minimum of a complex terrain of possible string solutions dominated by hills and valleys. This terrain has come to be known as the “string-theory landscape” [1].

The existence of such a landscape has tremendous practical significance because the specific low-energy phenomenology that can be expected to emerge from string theory depends critically on the particular choice of vacuum state. Detailed quantities such as particle masses and mixings, and even more general quantities and structures such as the choice of gauge group, number of chiral particle generations, magnitude of the supersymmetry-breaking scale, and even the cosmological constant can be expected to vary significantly from one vacuum solution to the next. Thus, in the absence of some sort of vacuum selection principle, it is natural to tackle a secondary but perhaps more tractable question concerning whether there might exist generic string-derived *correlations* between different phenomenological features. In this way, one can still hope to extract phenomenological predictions from string theory.

This idea has triggered a recent surge of activity concerning the *statistical* properties of the landscape [2–13]. Investigations along these lines have focused on diverse phenomenological issues, including the value of the supersymmetry-breaking scale [2, 3], the value of the cosmological constant [7, 8, 9], and the preferred rank of the corresponding gauge groups, the prevalence of the Standard-Model gauge group, and possible numbers of chiral generations [2, 5, 6]. Discussions of the landscape have also led to various theoretical paradigm shifts, ranging from alternative landscape-based notions of naturalness [3, 4] and novel cosmological inflationary scenarios [7, 8, 9] to the use of anthropic arguments to constrain the set of viable string vacua [7, 9, 12]. There have even been proposals for field-theoretic analogues of the string-theory landscape [11] as well as discussions concerning whether there truly exist effective field theories that can describe it [13]. Collectively, these developments

have even given birth to a large, ambitious, organized effort dubbed the “String Vacuum Project (SVP)” [15], one of whose purposes is to map out the properties of this landscape of string vacua. It is envisioned that this will happen not only through direct enumeration/construction of viable string vacua, but also through planned large-scale statistical studies across the landscape as a whole.

Unfortunately, although there have been many abstract theoretical discussions of such vacua and their statistical properties, there have been relatively few direct statistical examinations of actual string vacua. Despite considerable effort, there have been relatively few pieces of actual data gleaned from direct studies of the string landscape and the vacua which populate it. This is because, in spite of recent progress, the construction and analysis of completely stable string vacua remains a rather complicated affair [16, 17]. Surveying whole classes of such vacua and doing a proper statistical analysis thus remains a formidable task.

There are exceptions, however. For example, one recent computer analysis examined millions of supersymmetric intersecting D-brane models on a particular orientifold background [5]. Although the models which were constructed for such analyses are not completely stable (since they continue to have flat directions), the analysis reported in Ref. [5] examined important questions such as the statistical occurrences of various gauge groups, chirality, numbers of generations, and so forth. A similar statistical study focusing on Gepner-type orientifolds exhibiting chiral supersymmetric Standard-Model spectra was performed in Ref. [6]. By means of such studies, a number of interesting statistical correlations were uncovered.

To date, however, there has been almost no discussion of the *heterotic* landscape. This is somewhat ironic, especially since perturbative heterotic strings were the framework in which most of the original work in string phenomenology was performed in the late 1980’s and early 1990’s.

In this paper, we shall present the results of the first statistical study of the heterotic string landscape. Thus, in some sense, this work can be viewed as providing a heterotic analogue of the work reported in Refs. [5, 6]. In this paper, we shall focus on a sample of approximately 1.2×10^5 distinct four-dimensional perturbative heterotic string models, all randomly generated, and we shall analyze statistical information concerning their gauge groups and one-loop cosmological constants.

As we shall see, the statistical properties of perturbative heterotic strings are substantially different from those of Type I strings. This is already apparent at the level of gauge groups: while the gauge groups of Type I strings are constrained only by allowed D-brane configurations and anomaly-cancellation constraints, those of perturbative heterotic strings necessarily have a maximum rank. Moreover, as we shall repeatedly see, modular invariance shall also prove to play an important role in constraining the features of the heterotic landscape. This too is a feature that is lacking for Type I landscape. On the other hand, there will be certain similarities. For example, one of our results will concern a probability for randomly obtaining the Standard-Model gauge group from perturbative heterotic strings. Surprisingly, this

probability shall be very close to what is obtained for Type I strings.

For various technical and historical reasons, our statistical study will necessarily have certain limitations. There will be discussed more completely below and in Sect. 2. However, three limitations are critical and deserve immediate mention.

First, as mentioned, our sample size is relatively small, consisting of only $\sim 10^5$ distinct models. However, although this number is miniscule compared with the numbers of string models that are currently quoted in most landscape discussions, we believe that the statistical results we shall obtain have already achieved saturation — *i.e.*, we do not believe that they will change as more models are added. We shall discuss this feature in more detail in Sect. 2.

Second, for historical reasons to be discussed below, our statistical study in this paper shall be limited to only two phenomenological properties of these models: their low-energy gauge groups, and their one-loop vacuum amplitudes (cosmological constants). Nevertheless, as we shall see, this represents a considerable wealth of data. Further studies are currently underway to investigate other properties of these models and their resulting spacetime spectra, and we hope to report those results in a later publication.

Perhaps most importantly, however, all of the models we shall be analyzing are non-supersymmetric. Therefore, even though they are all tachyon-free, they have non-zero dilaton tadpoles and thus are not stable beyond tree level. Indeed, the models we shall be examining can be viewed as four-dimensional analogues of the $SO(16) \times SO(16)$ heterotic string in ten dimensions [18]. Such models certainly satisfy all of the necessary string self-consistency constraints — they have worldsheet conformal/superconformal invariance, they have one-loop and multi-loop modular-invariant amplitudes, they exhibit proper spin-statistics relations, and they contain physically sensible GSO projections and orbifold twists. However, they are not stable beyond tree level.

Clearly, such models do not represent the sorts of truly stable vacua that we would ideally like to be studying. Again invoking landscape imagery, such models do not sit at local minima in the landscape — they sit on hillsides and mountain passes, valleys and even mountaintops. Thus, in this paper, we shall in some sense be surveying the entire *profile* of the landscape rather than merely the properties of its local minima. Indeed, we can call this a “raindrop” study: we shall let the rain fall randomly over the perturbative heterotic landscape and collect statistical data where each raindrop hits the surface. Clearly this is different in spirit from a study in which our attention is restricted to the locations of the puddles which remain after the rain has stopped and the sun comes out.

Despite these limitations, we believe that such a study can be of considerable value. First, such models do represent valid string solutions at tree level, and it is therefore important to understand their properties as a first step towards understanding the full phenomenology of non-supersymmetric strings and their contributions to the overall architecture of the landscape. Indeed, since no stable perturbative non-

supersymmetric heterotic strings have yet been constructed, our study represents the current state of the art in the statistical analysis of perturbative non-supersymmetric heterotic strings.

Second, as we shall discuss further in Sect. 2, the models we shall be examining range from the extremely simple, involving a single set of sectors, to the extraordinarily complex, involving many convoluted layers of overlapping orbifold twists and Wilson lines. In all cases, these sets of orbifolds twists and Wilson lines were randomly generated, yet each satisfies all necessary self-consistency constraints. These models thus exhibit an unusual degree of intricacy and complexity, just as we expect for models which might eventually exhibit low-energy phenomenologies resembling that of the real world.

Third, an important question for any landscape study is to understand the phenomenological roles played by supersymmetry and by the need for vacuum stability. However, the only way in which we might develop an understanding of the statistical significance of the effects that spacetime supersymmetry might have on other phenomenological properties (such as gauge groups, numbers of chiral generations, *etc.*) is to already have the results of a study of strings in which supersymmetry is absent.

But most importantly, we know as an experimental fact that the low-energy world is non-supersymmetric. Therefore, if we believe that perturbative heterotic strings are relevant to its description, it behooves us to understand the properties of non-supersymmetric strings. Although no such strings have yet been found which are stable beyond tree level, analyses of these unstable vacua may prove useful in pointing the way towards their eventual constructions. Indeed, as we shall see, some of our results shall suggest some of the likely phenomenological properties that such string might ultimately have.

This paper is organized as follows. In Sect. 2, we shall provide an overview of the models that we will be analyzing in this paper. We shall also discuss, in more detail, the limitations and methodologies of our statistical study. In Sect. 3, we shall then provide a warm-up discussion that focuses on the better-known properties of the *ten*-dimensional heterotic landscape. We will then turn our attention to heterotic strings in four dimensions for the remainder of the paper. In Sect. 4, we shall focus on the gauge groups of such strings, and in Sect. 5 we shall focus on their one-loop vacuum energies (cosmological constants). Finally, in Sect. 6, we shall analyze the statistical *correlations* between the gauge groups and cosmological constants. A short concluding section will then outline some future directions. Note that even though these string models are unstable beyond tree level, we shall use the terms “string models” and “string vacua” interchangeably in this paper to refer to these non-supersymmetric, tachyon-free string solutions.

Historical note

This paper has a somewhat unusual provenance. Therefore, before beginning, we provide a brief historical note.

In the late 1980's, soon after the development of the free-fermionic construction [19], a number of string theorists undertook various computer-automated randomized searches through the space of perturbative four-dimensional heterotic string models. The most detailed and extensive of such searches was described in Ref. [20]; to the best of our knowledge, this represents the earliest automated search through the space of heterotic string models. Soon afterwards, other searches were also performed (see, *e.g.*, Ref. [21]).

At that time, the goals of such studies were to find string models with certain favorable phenomenological properties. In other words, these investigations were viewed as searches rather than as broad statistical studies.

One such search at that time [21] was aimed at finding four-dimensional perturbative non-supersymmetric tachyon-free heterotic string models which nevertheless have zero one-loop cosmological constants. Inspired by Atkin-Lehner symmetry and its possible extensions [22], we conducted a search using the techniques (and indeed some of the software) first described in Ref. [20]. At that time, our interest was purely on the values of the cosmological constant. However, along the way, the corresponding gauge groups of these models were also determined and recorded.

In this paper, we shall report on the results of a new, comprehensive, statistical analysis of this “data” which was originally collected in the late 1980's. As a consequence of the limited scope of our original search, our statistical analysis here shall therefore be focused on non-supersymmetric tachyon-free models. Likewise, in this paper we shall concentrate on only the two phenomenological properties of such models (gauge groups and cosmological constants) for which such data already existed. As mentioned above, a more exhaustive statistical study using modern software and a significantly larger data set is currently underway: this will include both supersymmetric and non-supersymmetric heterotic string models, and will involve many additional properties of the physical spectra of the associated models (including their gauge groups, numbers of generations, chirality properties, and so forth). However, the study described in this paper shall be limited to the data set that was generated as part of the investigations of Ref. [21]. Although this data was generated over fifteen years ago, we point out that almost all of statistical results of this paper were obtained recently and have not been published or reported elsewhere in the string literature.

2 The string vacua examined

In this section we shall describe the class of string vacua which are included in our statistical analysis.

Each of these vacua represents a weakly coupled critical heterotic string compactified to, or otherwise constructed directly in, four large (flat) spacetime dimensions. In general, such a string may be described in terms of its left- and right-moving worldsheet conformal field theories (CFT's); in four dimensions, in addition to the

spacetime coordinates and their right-moving worldsheet superpartners, these internal CFT's must have central charges $(c_R, c_L) = (9, 22)$ in order to enforce worldsheet conformal anomaly cancellation. While the left-moving internal CFT must merely exhibit conformal invariance, the right-moving internal CFT must actually exhibit superconformal invariance. While any CFT's with these central charges may be considered, in this paper we shall focus on those string models for which these internal worldsheet CFT's may be taken to consist of tensor products of free, non-interacting, complex (chiral) bosonic or fermionic fields.

This is a huge class of models which has been discussed and analyzed in many different ways in the string literature. On the one hand, taking these worldsheet fields as fermionic leads to the so-called “free-fermionic” construction [19] which will be our primary tool throughout this paper. In the language of this construction, different models are achieved by varying (or “twisting”) the boundary conditions of these fermions around the two non-contractible loops of the worldsheet torus while simultaneously varying the phases according to which the contributions of each such spin-structure sector are summed in producing the one-loop partition function. However, alternative but equivalent languages for constructing such models exist. For example, we may bosonize these worldsheet fermions and construct “Narain” models [23, 24] in which the resulting complex worldsheet bosons are compactified on internal lattices of appropriate dimensionality with appropriate self-duality properties. Furthermore, many of these models have additional geometric realizations as orbifold compactifications with randomly chosen Wilson lines; in general, the process of orbifolding is quite complicated in these models, involving many sequential layers of projections and twists. Note that all of these constructions generally overlap to a large degree, and all are capable of producing models in which the corresponding gauge groups and particle contents are quite intricate. Nevertheless, in all cases, we must ensure that all required self-consistency constraints are satisfied. These include modular invariance, physically sensible GSO projections, proper spin-statistics identifications, and so forth. Thus, each of these vacua represents a fully self-consistent string solution at tree level.

In order to efficiently survey the space of such non-supersymmetric four-dimensional string-theoretic vacua, we implemented a computer search based on the free-fermionic spin-structure construction, as originally developed in Ref. [19]. Recall that in this light-cone gauge construction, each of the six compactified bosonic spacetime coordinates is fermionized to become two left-moving and two right-moving internal free real fermions, and consequently our four-dimensional heterotic strings consist of the following fields on the worldsheet: 20 right-moving free real fermions (the eight original supersymmetric partners of the eight transverse bosonic coordinates of the ten-dimensional string, along with twelve additional internal fermions resulting from compactification); 44 left-moving free real fermions (the original 32 in ten dimensions plus the additional twelve resulting from compactification); and of course the two transverse bosonic (coordinate) fields X^μ . Of these 20 right-moving

real fermions, only two (the supersymmetric partners of the two remaining transverse coordinates) carry Lorentz indices. In our analysis, we restricted our attention to those models for which our real fermions can always be uniformly paired to form complex fermions, and therefore it was possible to specify the boundary conditions (or spin-structures) of these real fermions in terms of the complex fermions directly. We also restricted our attention to cases in which the worldsheet fermions exhibited either antiperiodic (Neveu-Schwarz) or periodic (Ramond) boundary conditions. Of course, in order to build a self-consistent string model in this framework, these boundary conditions must satisfy tight constraints. These constraints are necessary in order to ensure that the one-loop partition function is modular invariant and that the resulting Fock space of states can be interpreted as arising from a physically sensible projection from the space of all worldsheet states onto the subspace of physical states with proper spacetime spin-statistics. Thus, within a given string model, it is necessary to sum over appropriate sets of untwisted and twisted sectors with different boundary conditions and projection phases.

Our statistical analysis consisted of an examination of 123,573 distinct vacua, each randomly generated through the free-fermionic construction. (In equivalent orbifold language, each vacuum was constructed from randomly chosen sets of orbifold twists and Wilson lines, subject to the constraints described above.) Details of this study are similar to those of the earlier study described in Ref. [20], and made use of model-generating software borrowed from that earlier study. Essentially, each set of boundary conditions was chosen randomly in each sector, subject only to the required self-consistency constraints. However, in our statistical sampling, we placed no limits on the complexity of the orbifold twisting (*i.e.*, on the number of basis vectors in the free-fermionic language). Thus, our statistical analysis included models of arbitrary intricacy and sophistication.

As discussed above, for the purpose of this search, we demanded that supersymmetry be broken without introducing tachyons. Thus, these vacua are all non-supersymmetric but tachyon-free, and can be considered as four-dimensional analogues of the ten-dimensional $SO(16) \times SO(16)$ heterotic string [18] which is also non-supersymmetric but tachyon-free. As a result, these models all have non-vanishing but finite one-loop cosmological constants/vacuum energies Λ , and we shall examine these values of Λ in Sect. 5. However, other than demanding that supersymmetry be broken in a tachyon-free manner, we placed no requirements on other possible phenomenological properties of these vacua such as the possible gauge groups, numbers of chiral generations, or other aspects of the particle content. We did, however, require that our string construction begin with a supersymmetric theory in which the supersymmetry is broken only through subsequent orbifold twists. (In the language of the free-fermionic construction, this is tantamount to demanding that our fermionic boundary conditions include a superpartner sector, typically denoted \mathbf{W}_1 or \mathbf{V}_1 .) This is to be distinguished from a potentially more general class of models in which supersymmetry does not appear at any stage of the construction. This is merely a

technical detail in our construction, and we do not believe that this ultimately affects our results.

Because of the tremendous redundancy inherent in the free-fermionic construction, string vacua were judged to be distinct based on their spacetime characteristics — *i.e.*, their low-energy gauge groups and massless particle content. Thus, as a minimum condition, distinct string vacua necessarily exhibit different massless spacetime spectra.* As we shall discuss further below, such a requirement about the distinctness of the spacetime spectrum must be an important component of any statistical study of string models. Since the same string model may have a plethora of different worldsheet realizations, one cannot verify that one is accurately surveying the space of distinct, independent string models based on their worldsheet realizations alone. This “redundancy” issue becomes increasingly pressing as larger and larger numbers of models are considered.

Clearly, this class of string models is not all-encompassing. By its very nature, the free-fermionic construction reaches only certain specific points in the full space of self-consistent string models. For example, since each worldsheet fermion is nothing but a worldsheet boson compactified at a specific radius, a larger (infinite) class of models can immediately be realized through a bosonic formulation by varying these radii away from their free-fermionic values. However, this larger class of models will typically have only abelian gauge groups and consequently uninteresting particle representations. Indeed, the free-fermionic points typically represent precisely those points at which additional (non-Cartan) gauge-boson states become massless, thereby enhancing the gauge symmetries to become non-abelian. Thus, the free-fermionic construction naturally leads to precisely the set of models which are likely to be of direct phenomenological relevance.

Similarly, it is possible to go beyond the class of free-field string models altogether, and consider models built from more complicated worldsheet CFT’s (*e.g.*, Gepner models). We may even transcend the realm of critical string theories, and consider non-critical strings and/or strings with non-trivial background fields. Likewise, we may consider heterotic strings beyond the usual perturbative limit. However, although such models may well give rise to phenomenologies very different from those that emerge in free-field constructions, their spectra are typically very difficult to analyze and are thus not amenable to an automated statistical investigation. Finally, even within the specific construction we are employing in this paper, we may drop our requirement that our models be non-supersymmetric, and consider models with varying degrees of unbroken supersymmetry. This will be done in future work.

*As a result of conformal invariance and modular invariance (both of which simultaneously relate states at all mass levels), it is extremely difficult for two string models to share the same massless spectrum (as well as the same off-shell tachyonic structure) and yet differ in their massive spectra. Thus, for all practical purposes, our requirement that two models must have different massless spectra is not likely to eliminate potential models whose spectra might differ only at the massive level.

Finally, we should point out that strictly speaking, the class of models we are considering is only finite in size. Because of the tight worldsheet self-consistency constraints arising from modular invariance and the requirement of physically sensible GSO projections, there are only a finite number of distinct boundary condition vectors and GSO phases which may be chosen in our construction as long as we restrict our attention to complex worldsheet fermions with only periodic (Ramond) or antiperiodic (Neveu-Schwarz) boundary conditions. For example, in four dimensions there are a maximum of only 32 boundary-condition vectors which can possibly be linearly independent, even before we impose other dot-product modular-invariance constraints.

This is, nevertheless, a very broad and general class of theories. Indeed, models which have been constructed using such techniques span almost the entire spectrum of closed-string models, including MSSM-like models, models with and without extra exotic matter, and so forth. Moreover, worldsheet bosonic and fermionic constructions can produce models which have an intricacy and complexity which is hard to duplicate purely through geometric considerations — indeed, these are often models for which no geometric compactification space is readily apparent. It is for this reason that while most of our geometric insights about string models have historically come from Calabi-Yau and general orbifold analyses, much of the serious work at realistic closed-string model-building over the past two decades has been through the more algebraic bosonic or fermionic formulations. It is therefore within this class of string models that our analysis will be focused. Moreover, as we shall see, this set of models is still sufficiently large to enable various striking statistical correlations to appear.

Finally, we provide some general comments about the statistical analysis we will be performing and the interpretation of our results.

As with any statistical landscape study, it is important to consider whether the properties we shall find are rigorously true for the landscape as a whole, or are merely artifacts of having considered only a finite statistical sample of models or a sample which is itself not representative of the landscape at large because it is statistically biased or skewed in some way. Clearly, without detailed analytical knowledge of the entire landscape of models in the category under investigation, one can never definitively answer this question. Thus, in each case, it is necessary to judge which properties or statistical correlations are likely to exist because of some deeper, identifiable string consistency constraint, and which are not. In this paper, we shall try to indicate in every circumstance what we believe are the appropriate causes of each statistical correlation we find.

The issue concerning the finite size of our sample is particularly relevant in our case, since we will be examining the properties of only $\sim 10^5$ distinct models in this paper. Although this is certainly a large number of string models on an absolute scale, this number is extremely small compared with the current estimated size of the entire string landscape. However, one way to judge the underlying validity of a particular statistical correlation is to test whether it persists without significant

modification as our sample size increases. If so, then it is likely that we have already reached the “continuum limit” (borrowing a phrase from our lattice gauge theory colleagues) as far as the particular statistical correlation is concerned. This can be verified by testing the numerical stability of a given statistical correlation as more and more string models are added to our sample set, and can be checked *a posteriori* by examining whether the correlation persists even if the final sample set is partitioned or subdivided. All correlations that we will present in this paper are stable in the “continuum limit” unless otherwise indicated.

Finally, we point out that all correlations in this paper will ultimately depend on a particular assumed measure across the landscape. For example, when we plot a correlation between two quantities, the averaging for these quantities is calculated across all models in our data set, with each physically distinct string model weighted equally. However, we expect that such averages would change significantly if models were weighted in a different manner. For example, as we shall see, many of our results would be altered if we were to weight our probabilities equally across the set of distinct gauge groups rather than across the set of distinct string models. This sensitivity to the underlying string landscape measure is, of course, well known. In this paper, we shall employ a measure in which each distinct string model is weighted equally across our sample set.

3 A preliminary example: The ten-dimensional heterotic landscape

Before plunging into the four-dimensional case of interest, let us first consider the “landscape” of *ten*-dimensional heterotic string models. Recall that in ten dimensions, such models have maximal gauge-group rank 16, corresponding to sixteen left-moving worldsheet bosons (or complex fermions).

It turns out that we can examine the resulting “landscape” of such models by arranging them in the form of a family “tree”. First, at the root of the tree, we have what is literally the simplest ten-dimensional heterotic string model we can construct: this is the supersymmetric $SO(32)$ heterotic string model in which our worldsheet fermionic fields all have identical boundary conditions in each spin-structure sector of the theory. Indeed, the internal $SO(32)$ rotational invariance amongst these fermions is nothing but the spacetime gauge group of the resulting model.

Starting from this model, there are then a number of ways in which we may “twist” the boundary conditions of these fields (or, in orbifold language, mod out by discrete symmetries). First, we might seek to twist the boundary conditions of these sixteen complex fermions into two blocks of eight complex fermions each. If we do this in a way that also breaks spacetime supersymmetry, we obtain a non-supersymmetric, tachyon free model with gauge group $SO(16) \times SO(16)$; in orbifold language, we have essentially chosen a SUSY-breaking orbifold which projects out

the non-Cartan gauge bosons in the coset $SO(32)/[SO(16) \times SO(16)]$. However, if we try to do this in a way which simultaneously preserves spacetime supersymmetry, we find that we cannot obtain $SO(16) \times SO(16)$; instead, modular invariance requires that our SUSY-preserving orbifold twist simultaneously come with a twisted sector which supplies new gauge-boson states, enhancing this gauge group to $E_8 \times E_8$. This produces the well-known $E_8 \times E_8$ heterotic string. The $SO(16) \times SO(16)$ and $E_8 \times E_8$ heterotic strings may thus be taken to sit on the second branch of our family tree.

Continuing from these three heterotic strings, we may continue to perform subsequent orbifold twists and thereby generate additional models. For example, we may act with other configurations of \mathbb{Z}_2 twists on the supersymmetric $SO(32)$ string model: the three other possible self-consistent models that can be obtained this way are the non-supersymmetric $SO(32)$ heterotic string model, the $SO(8) \times SO(24)$ string model, and a heterotic string model with gauge group $U(16) = SU(16) \times U(1)$. All have physical (on-shell) tachyons in their spectrum. Likewise, we may perform various \mathbb{Z}_2 orbifolds of the $E_8 \times E_8$ string model: self-consistent choices produce additional non-supersymmetric, tachyonic models with gauge groups $SO(16) \times E_8$ and $(E_7)^2 \times SU(2)^2$. Finally, we may also orbifold the $E_8 \times E_8$ model by a discrete symmetry (outer automorphism) which exchanges the two E_8 gauge groups, producing a final non-supersymmetric, tachyonic (rank-reduced) model with a single E_8 gauge group realized at affine level $k = 2$ [25]. By its very nature, this last model is beyond the class of models with complex worldsheet fields that we will be considering, since modding out by the outer automorphism cannot be achieved on the worldsheet except through the use of *real* worldsheet fermions, or by employing non-abelian orbifold techniques.

In this manner, we have therefore generated the nine self-consistent heterotic string models in ten dimensions which are known to completely fill out the ten-dimensional heterotic “landscape” [25]. However, the description we have provided above represents only one possible route towards reaching these nine models; other routes along different branches of the tree are possible. For example, the non-supersymmetric, tachyon-free $SO(16) \times SO(16)$ heterotic string can be realized either as a \mathbb{Z}_2 orbifold of the supersymmetric $SO(32)$ string or as a different \mathbb{Z}_2 orbifold of the $E_8 \times E_8$ string. Thus, rather than a direct tree of ancestors and descendants, what we really have are deeply interlocking webs of orbifold relations.

A more potent example of this fact is provided by the single- E_8 heterotic string model. This model can be constructed through several entirely different constructions: as a free-fermionic model involving necessarily real fermions; as an abelian orbifold of the $E_8 \times E_8$ heterotic string model in which the discrete symmetry is taken to be an outer automorphism (exchange) of the two E_8 gauge symmetries; and as a *non*-abelian orbifold model in which the non-abelian discrete group is D_4 [26]. Moreover, as noted above, even within a given construction numerous unrelated combinations of parameter choices can yield exactly the same string model. These sorts of redundancy issues become increasingly relevant as larger and larger sets of models

are generated and analyzed, and must be addressed in order to allow efficient progress in the task of enumerating models.

One way to categorize different branches of the “tree” of models is according to total numbers of irreducible gauge-group factors that these models contain. As we have seen, the ten-dimensional heterotic landscape contains exactly three models with only one irreducible gauge group: these are the $SO(32)$ models, both supersymmetric and non-supersymmetric, and the single- E_8 model. By contrast, there are five models with two gauge-group factors: these are the models with gauge groups $E_8 \times E_8$, $SO(16) \times SO(16)$, $SO(24) \times SO(8)$, $SU(16) \times U(1)$, and $SO(16) \times E_8$. Finally, there is one model with four gauge-group factors: this is the $(E_7)^2 \times SU(2)^2$ model. Note that no other models with other numbers of gauge-group factors appear in ten dimensions. Alternatively, we may classify our models into groups depending on their spacetime supersymmetry properties: there are two models with unbroken spacetime supersymmetry, one with broken supersymmetry but without tachyons, and six with both broken supersymmetry and tachyons.

Clearly, this ten-dimensional heterotic “landscape” is very restricted, consisting of only nine discrete models. Nevertheless, many of the features we shall find for the four-dimensional heterotic landscape are already present here:

- First, we observe that not all gauge groups can be realized. For example, we do not find any ten-dimensional heterotic string models with gauge group $SO(20) \times SO(12)$, even though this gauge group would have the appropriate total rank 16. We also find no models with three gauge-group factors, even though we have models with one, two, and four such factors. Indeed, of all possible gauge groups with total rank 16 that may be constructed from the simply-laced factors $SO(2n)$, $SU(n)$ and $E_{6,7,8}$, we see that only eight distinct combinations emerge from the complete set of self-consistent string models. Likewise, if we allow for the possibility of a broader class of models which incorporate rank-cutting, then we must also allow for the possibility that our gauge group can be composed of factors which also include the non-simply laced gauge groups $SO(2n+1)$, $Sp(2n)$, F_4 , and G_2 . However, even from this broader set, only one additional gauge group (a single E_8) is actually realized.
- Second, we see that certain phenomenological features are *correlated* in such strings. For example, although there exist models with gauge groups $SO(16) \times SO(16)$ and $E_8 \times E_8$, the first gauge group is possible only in the non-supersymmetric case, while the second is possible only in the supersymmetric case. These two features (the presence/absence of spacetime supersymmetry and the emergence of different possible gauge groups) are features that would be completely disconnected in quantum field theory, and thus represent intrinsically *stringy correlations*. As such, these may be taken to represent statistical predictions from string theory, manifestations of the deeper worldsheet self-consistency constraints that string theory imposes.

- Third, we have seen that a given string model can be realized in many different ways on the worldsheet, none of which is necessarily special or preferred. This is part of the huge redundancy of string constructions that we discussed in Sect. 2. Thus, all of the string models that we shall discuss will be defined to be physically distinct on the basis of their *spacetime* properties (*e.g.*, on the basis of differing spacetime gauge groups or particle content).
- Fourth, we see that our ten-dimensional “landscape” contains models with varying amounts of supersymmetry: in ten dimensions, we found $\mathcal{N} = 1$ supersymmetric models, non-supersymmetric tachyon-free models, and non-supersymmetric models with tachyons. These are also features which will survive into the heterotic landscapes in lower dimensions, where larger numbers of unbroken supersymmetries are also possible. Since other phenomenological properties of these models may be correlated with their degrees of supersymmetry, it is undoubtedly useful to separate models according to this primary feature before undertaking further statistical analyses.
- Finally, we observe that a heterotic string model with the single rank-eight gauge group E_8 is already present in the ten-dimensional heterotic landscape. This is a striking illustration of the fact that not all string models can be realized through orbifold techniques of the sort we will be utilizing, and that our landscape studies will necessarily be limited in both class and scope.

4 Gauge groups: Statistical results

We now turn our attention to our main interest, the landscape of heterotic string models in four dimensions. As we discussed in Sect. 2, the string models we are examining are free-field models (*i.e.*, models in which our worldsheet fields are free and non-interacting). As such, the gauge sector of such four-dimensional heterotic string models can be described by even self-dual* Lorentzian lattices of dimensionality $(6, 22)$, as is directly evident in a bosonic (Narain) construction [23, 24]. [This is the four-dimensional analogue of the sixteen-dimensional lattice that underlies the $SO(32)$ or $E_8 \times E_8$ heterotic string models in ten dimensions; the remaining $(6, 6)$ components arise internally through compactification from ten to four dimensions.] In general, the right-moving (worldsheet supersymmetric) six-dimensional components of these gauge lattices correspond at best to very small right-moving gauge groups composed of products of $U(1)$ ’s, or $SU(2)$ ’s realized at affine level $k = 2$. We shall therefore disregard these right-moving gauge groups and focus exclusively on the left-moving gauge groups of these models. Moreover, because we are focusing on

*For strings with spacetime supersymmetry, modular invariance requires these gauge lattices to be even and self-dual. In other cases, the self-duality properties actually apply to the full lattice corresponding to the internal gauge group as well as the spacetime Lorentz group.

free-field constructions involving only complex bosonic or fermionic worldsheet fields, the possibility of rank-cutting is not available in these models. Consequently, these models all have left-moving simply-laced gauge groups with total rank 22, realized at affine level $k = 1$.

As we shall see, the twin requirements of modular invariance and physically sensible projections impose powerful self-consistency constraints on such models and their possible gauge groups. As such, these are features that are not present for open strings, but they are ultimately responsible for most of the statistical features we shall observe. Moreover, as discussed previously, in this paper we shall restrict our attention to models which are non-supersymmetric but tachyon-free. Such models are therefore stable at tree level, but have finite, non-zero one-loop vacuum energies (one-loop cosmological constants).

In this section, we shall focus on statistical properties of the gauge groups of these models. We believe that these properties are largely independent of the fact that our models are non-supersymmetric. In Sect. 5, we shall then focus on the statistical distributions of the values of their cosmological constants, and in Sect. 6 we shall discuss correlations between the gauge groups and the cosmological constants.

In comparison with the situation for heterotic strings in ten dimensions, the four-dimensional situation is vastly more complex, with literally billions and billions of distinct, self-consistent heterotic string models exhibiting arbitrary degrees of intricacy and complexity. These models are generated randomly, with increasingly many randomly chosen twists and overlapping orbifold projections. Each time a self-consistent model is obtained, it is compared with all other models that have already been obtained. It is deemed to represent a new model only if it has a massless spacetime spectrum which differs from all models previously obtained. Because of the tremendous worldsheet redundancy inherent in the free-fermionic approach, it becomes increasingly more difficult (both algorithmically and in terms of computer time) to find a “new” model as more and more models are constructed and stored. Nevertheless, through random choices for all possible twists and GSO projection phases, we have generated a set of more than 10^5 distinct four-dimensional heterotic string models which we believe provide a statistically representative sample of the heterotic landscape. Indeed, in many cases we believe that our sample is essentially complete, especially for relatively simple models involving relatively few orbifold twists.

Just as for ten-dimensional heterotic strings, we can visualize a “tree” structure, grouping our models on higher and higher branches of the tree in terms of their numbers of gauge-group factors. For this purpose, we shall decompose our gauge groups into irreducible factors; *e.g.*, $SO(4) \sim SU(2) \times SU(2)$ will be considered to have two factors. We shall generally let f denote the number of irreducible gauge-group factors. Clearly, as f increases, our gauge group of total rank 22 becomes increasingly “shattered” into smaller and smaller pieces.

The following is a description of some salient features of the tree that emerges

from our study. Again we emphasize that our focus is restricted to models which are non-supersymmetric but tachyon-free.

- $f = 1$: We find that there is only one heterotic string model whose gauge group contains only one factor: this is an $SO(44)$ string model which functions as the “root” of our subsequent tree. This is a model in which all left-moving worldsheet fermions have identical boundary conditions, but in which all tachyons are GSO-projected out of the spectrum. This model is the four-dimensional analogue of the ten-dimensional $SO(32)$ heterotic string model.
- $f = 2$: On the next branch, we find 34 distinct string models whose gauge groups contain two simple factors. As might be expected, in all cases these gauge groups are of the form $SO(44 - n) \times SO(n)$ for $n = 8, 12, 16, 20$. Each of these models is constructed from the above $SO(44)$ string model by implementing a single twist. Modular invariance, together with the requirement of worldsheet superconformal invariance and a single-valued worldsheet supercurrent, are ultimately responsible for restricting the possible twists to those with $n = 8, 12, 16, 20$. Note that $n = 36, 32, 28, 24$ are implicitly included in this set, yielding the same gauge groups as those with $n = 8, 12, 16, 20$ respectively. Finally, note that cases with $n = 4$ (or equivalently $n = 40$) are not absent; they are instead listed amongst the $f = 3$ models since $SO(4) \sim SU(2) \times SU(2)$.
- $f = 3$: On the next branch, we find that 186 distinct models with eight distinct gauge groups emerge. Notably, this branch contains the first instance of an exceptional group. The eight relevant gauge groups, each with total rank 22, are: $SO(28) \times SO(8)^2$, $SO(24) \times SO(12) \times SO(8)$, $SO(20) \times SO(16) \times SO(8)$, $SO(20) \times SO(12)^2$, $SO(16)^2 \times SO(12)$, $SO(40)^2 \times SU(2)^2$, $E_8 \times SO(20) \times SO(8)$, and $E_8 \times SO(16) \times SO(12)$.
- $f = 4$: This level gives rise to 34 distinct gauge groups, and is notable for the first appearance of E_7 as well as the first appearance of non-trivial $SU(n)$ groups with $n = 4, 8, 12$. This is also the first level at which gauge groups begin to contain $U(1)$ factors. This correlation between $SU(n)$ and $U(1)$ gauge-group factors will be discussed further below. Note that other ‘SU’ groups are still excluded, presumably on the basis of modular-invariance constraints.
- $f = 5$: This is the first level at which E_6 appears, as well as gauge groups $SU(n)$ with $n = 6, 10, 14$. We find 49 distinct gauge groups at this level.

As we continue towards larger values of f , our gauge groups become increasingly “shattered” into more and more irreducible factors. As a result, it becomes more and more difficult to find models with relatively large gauge-group factors. Thus, as f increases, we begin to witness the disappearance of relatively large groups and a predominance of relatively small groups.

- $f = 6$: At this level, $SU(14)$ disappears while $SU(7)$ makes its first appearance. We find 70 distinct gauge groups at this level.
- $f = 7$: We find 75 distinct gauge groups at this level. Only one of these gauge groups contains an E_8 factor. This is also the first level at which an $SU(5)$ gauge-group factor appears.
- $f = 8$: We find 89 distinct gauge groups at this level. There are no E_8 gauge-group factors at this level, and we do not find an E_8 gauge-group factor again at any higher level. This also the first level at which an $SU(3)$ factor appears. Thus, assuming these properties persist for the full heterotic landscape, we obtain an interesting stringy correlation: no string models in this class can have a gauge group containing $E_8 \times SU(3)$. These sorts of constraints emerge from modular invariance — *i.e.*, our inability to construct a self-dual 22-dimensional lattice with these two factors. Indeed, such a gauge group would have been possible based on all other considerations (*e.g.*, CFT central charges, total rank constraints, *etc.*).
- $f = 9$: Here we find that our string models give rise to 86 distinct gauge groups. This level also witnesses the permanent disappearance of $SU(12)$.

This tree ends, of course, at $f = 22$, where our gauge groups contain only $U(1)$ and $SU(2)$ factors, each with rank 1. It is also interesting to trace the properties of this tree backwards from the $f = 22$ endpoint.

- $f = 22$: Here we find only 16 gauge groups, all of the form $U(1)^n \times SU(2)^{22-n}$ for all values $0 \leq n \leq 22$ except for $n = 1, 2, 3, 5, 7, 9, 11$. Clearly no larger gauge-group factors are possible at this “maximally shattered” endpoint.
- $f = 21$: Moving backwards one level, we find 10 distinct gauge groups, all of the form $U(1)^n \times SU(2)^{20-n} \times SU(3)$ for $n = 9, 11, 12, 13, 14, 15, 16, 17, 18, 19$. Note that at this level, an $SU(3)$ factor must *always* exist in the total gauge group since there are no simply-laced irreducible rank-two groups other than $SU(3)$.
- $f = 20$: Moving backwards again, we find 24 distinct gauge groups at this level. Each of these models contains either $SU(3)^2$ or $SU(4) \sim SO(6)$.
- $f = 19$: Moving backwards one further level, we find 37 distinct gauge groups, each of which contains either $SU(3)^3$ or $SU(3) \times SU(4)$ or $SU(5)$ or $SO(8)$.

Clearly, this process continues for all branches of our “tree” over the range $1 \leq f \leq 22$. Combining these results from all branches, we find a total of 1301 distinct gauge groups from amongst over 120,000 distinct models.

As we discussed at the end of Sect. 2, it is important in such a statistical landscape study to consider whether the properties we find are rigorously true or are merely artifacts of having considered a finite statistical sample of models or a sample which is itself not representative of the landscape at large. One way to do this is to determine which properties or statistical correlations are likely to persist because of some deeper string consistency constraint, and which are likely to reflect merely a finite sample size.

For example, the fact that the $f = 21, 22$ levels give rise to gauge groups of the forms listed above with only particular values of n is likely to reflect the finite size of our statistical sample. Clearly, it is extremely difficult to randomly find a sequence of overlapping sequential orbifold twists which breaks the gauge group down to such forms for any arbitrary values of n , all without introducing tachyons, so it is entirely possible that our random search through the space of models has simply not happened to find them all. Thus, such restrictions on the values of n in these cases are not likely to be particularly meaningful.

However, the broader fact that E_8 gauge-group factors are not realized beyond a certain critical value of f , or that $SU(3)$ gauge-group factors are realized only beyond a different critical value of f , are likely to be properties that relate directly back to the required self-duality of the underlying charge lattices. Such properties are therefore likely to be statistically meaningful and representative of the perturbative heterotic landscape as a whole. Of course, the quoted values of these critical values of f should be viewed as approximate, as statistical results describing probability distributions. Nevertheless, the relative appearance and disappearance of different gauge-group factors are likely to be meaningful. Throughout this paper, we shall focus on only those statistical correlations which we believe represent the perturbative heterotic landscape at large. Indeed, these correlations are stable in the “continuum limit” (in the sense defined at the end of Sect. 2).

Having outlined the basic tree structure of our heterotic mini-landscape, let us now examine its overall statistics and correlations. The first question we might ask pertains to the *overall distribution* of models across bins with different values of f . Just how “shattered” are the typical gauge groups in our heterotic landscape?

The results are shown in Fig. 1, where we plot the absolute probabilities of obtaining distinct four-dimensional heterotic string models as a function of f , the number of factors in their spacetime gauge groups. These probabilities are calculated by dividing the total number of distinct models that we have found for each value of f by the total number of models we have generated. (Note that we plot relative probabilities rather than raw numbers of models because it is only these relative probabilities which are stable in the continuum limit discussed above. Indeed, we have explicitly verified that restricting our sample size in any random manner does not significantly affect the overall shape of the curves in Fig. 1.) The average number of gauge-group factors in our sample set is $\langle f \rangle \approx 13.75$.

It is easy to understand the properties of these curves. For $f = 1$, we have only

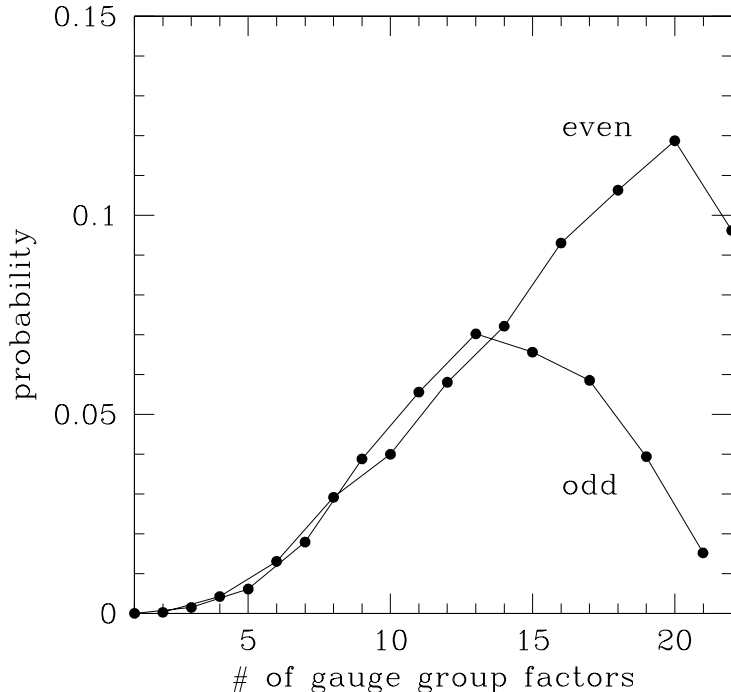


Figure 1: The absolute probabilities of obtaining distinct four-dimensional heterotic string models as a function of the degree to which their gauge groups are “shattered” into separate irreducible factors, stretching from a unique model with the irreducible rank-22 gauge group $SO(44)$ to models with only rank-one $U(1)$ and $SU(2)$ gauge-group factors. The total value of the points (the “area under the curve”) is 1. As the number of gauge-group factors increases, the behavior of the probability distribution bifurcates according to whether this number is even or odd. Indeed, as this number approaches its upper limit 22, models with even numbers of gauge-group factors become approximately ten times more numerous than those with odd numbers of gauge-group factors.

one string model, with gauge group $SO(44)$. However, as f increases beyond 1, the models grow in complexity, each with increasingly intricate patterns of overlapping orbifold twists and Wilson lines, and consequently the number of such distinct models grows considerably.

For $f \gtrsim 14$, we find that the behavior of this probability as a function of f bifurcates to whether f is even or odd. Indeed, as $f \rightarrow 22$, we find that models with even numbers of gauge-group factors become approximately ten times more numerous than those with odd numbers of gauge-group factors. Of course, this behavior might be an artifact of our statistical sampling methodology for randomly generating string models. However, we believe that this is actually a reflection of the underlying modular-invariance constraints that impose severe self-duality restrictions on the

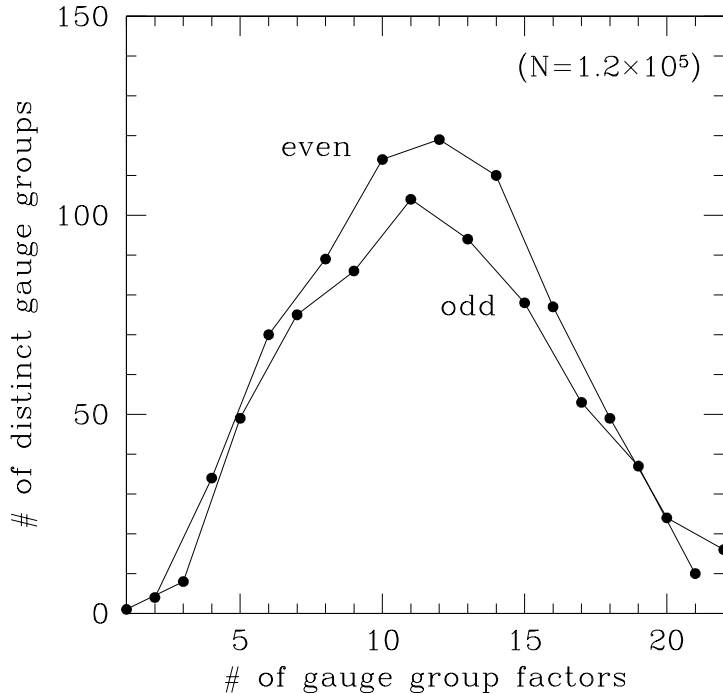


Figure 2: The number of distinct gauge groups realized from heterotic string models with f gauge-group factors, plotted as a function of f . Only 1301 distinct gauge groups are realized from $\sim 10^5$ distinct heterotic string models.

charge lattices corresponding to these models.

Fig. 1 essentially represents the total number of distinct *models* found as a function of f . However, we can also examine the number of distinct *gauge groups* found as a function of f . This data appears in Fig. 2. Once again, although we expect the raw number of distinct gauge groups for each f to continue to grow as our sample size increases, we do not expect the overall shape of these curves to change significantly. For small values of f , the number of distinct realizable gauge groups is relatively small, as discussed earlier. For example, for $f = 1$ we have a single realizable gauge group $SO(44)$, while for $f = 2$ we have the four groups $SO(44 - n) \times SO(n)$ for $n = 8, 12, 16, 20$. Clearly, as f increases, the number of potential gauge group combinations increases significantly, reaching a maximum for $f \approx 12$. Beyond this, however, the relative paucity of Lie groups with small rank becomes the dominant limiting factor, ultimately leading to very few distinct realizable gauge groups as $f \rightarrow 22$.

Since we have found that $N \approx 1.2 \times 10^5$ distinct heterotic string models yield only 1301 distinct gauge groups, this number of models yields an average gauge-group multiplicity factor ≈ 95 . As we shall discuss later (*c.f.* Fig. 10), we expect that this

multiplicity will only increase as more models are added to our sample set. However, it is also interesting to examine how this average multiplicity is distributed across the set of distinct gauge groups. This can be calculated by dividing the absolute probabilities of obtaining distinct heterotic string models (plotted as a function of f in Fig. 1) by the number of distinct gauge groups (plotted as a function of f in Fig. 2). The resulting average multiplicity factor, distributed as a function of f , is shown in Fig. 3. As we see, this average redundancy factor is relatively small for small f , but grows dramatically as f increases. This makes sense: as the heterotic gauge group accrues more factors, there are more combinations of allowed representations for our matter content, thereby leading to more possibilities for distinct models with distinct massless spectra.

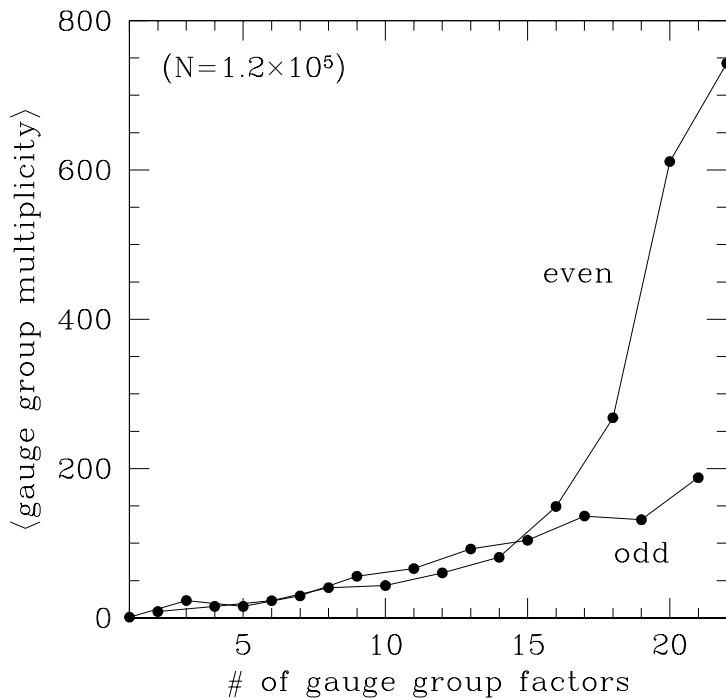


Figure 3: Average gauge-group multiplicity (defined as the number of distinct heterotic string models divided by the number of distinct gauge groups), plotted as a function of f , the number of gauge-group factors in the total gauge group. As the number of factors increases, we see that there are indeed more ways of producing a distinct string model with a given gauge group. Note that the greatest multiplicities occur for models with relatively large, *even* numbers of gauge-group factors.

Another important statistical question we may consider concerns the relative abundances of ‘SO’, ‘SU’, and exceptional gauge groups. Regardless of the value of f , the total rank of the full gauge group is 22; thus, the interesting question con-

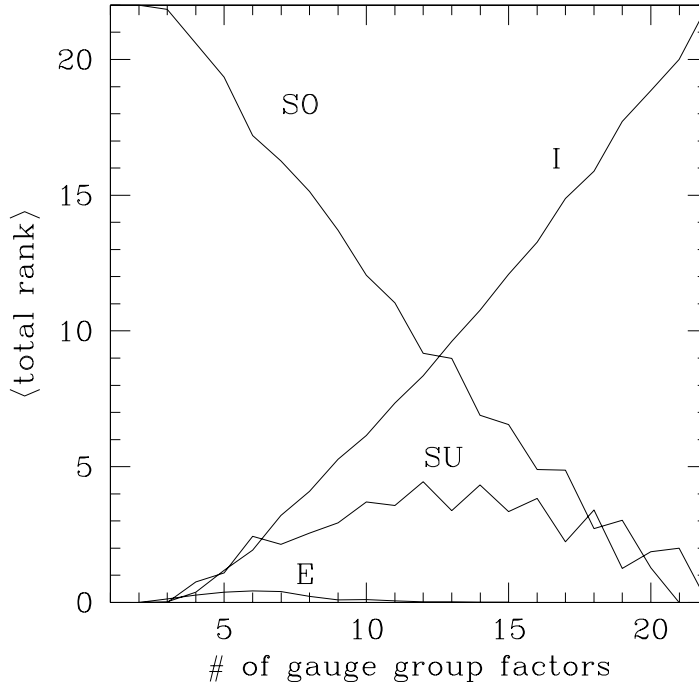


Figure 4: The composition of heterotic gauge groups, showing the average contributions to the total allowed rank from $SO(2n \geq 6)$ factors (denoted ‘SO’), $SU(n \geq 3)$ factors (denoted ‘SU’), exceptional group factors $E_{6,7,8}$ (denoted ‘E’), and rank-one factors $U(1)$ and $SU(2)$ (denoted ‘I’). In each case, these contributions are plotted as functions of the number of gauge-group factors in the string model and averaged over all string models found with that number of factors. In the case of $SU(4) \sim SO(6)$ factors, the corresponding rank contribution is apportioned equally between the ‘SO’ and ‘SU’ categories. The total of all four lines is 22, as required.

cerns how this total rank is apportioned amongst these different classes of Lie groups. This information is shown in Fig. 4. For the purposes of this plot, contributions from $SU(4) \sim SO(6)$ factors, when they occur, are equally shared between ‘SO’ and ‘SU’ categories. The total of all four lines is 22, as required. Once again, we observe several important features which are consistent with our previous discussions. First, we see that all of the allowed rank is found to reside in ‘SO’ groups for $f = 1, 2$; for $f = 1$, this is because the unique realizable gauge group in such models is $SO(44)$, while for $f = 2$, this is because the only realizable gauge-group breaking in such models is of the form $SO(44) \rightarrow SO(44 - n) \times SO(n)$ for $n = 8, 12, 16, 20$. We also observe that the ‘E’ groups do not contribute any net rank unless $f \geq 3$, while the ‘SU’ groups do not contribute any net rank unless $f \geq 4$. It is worth noting that the exceptional groups $E_{6,7,8}$ are exceedingly rare for all values of f , especially given that

their share of the total rank in a given string model must be at least six whenever they appear. As f grows increasingly large, however, the bulk of the rank is to be found in $U(1)$ and $SU(2)$ gauge factors. Of course, for $f = 21$, the ‘SU’ groups have an average rank which is exactly equal to 2. This reflects the fact that each of the realizable gauge groups for $f = 21$ necessarily contains a single $SU(3)$ factor, as previously discussed.

Across all of our models, we find that

- **85.79%** of our heterotic string models contain $SO(2n \geq 6)$ factors; amongst these models, the average number of such factors is ≈ 2.5 .
- **74.35%** of our heterotic string models contain $SU(n \geq 3)$ factors; amongst these models, the average number of such factors is ≈ 2.05 .
- **0.57%** of our heterotic string models contain $E_{6,7,8}$ factors; amongst these models, the average number of such factors is ≈ 1.01 .
- **99.30%** of our heterotic string models contain $U(1)$ or $SU(2)$ factors; amongst these models, the average number of such factors is ≈ 13.04 .

In the above statistics, an $SU(4) \sim SO(6)$ factor is considered to be a member of whichever category (‘SU’ or ‘SO’) is under discussion.

Note that these statistics are calculated across distinct heterotic string models. However, as we have seen, there is a tremendous redundancy of gauge groups amongst these string models, with only 1301 distinct gauge groups appearing for these $\approx 1.2 \times 10^5$ models. Evaluated across the set of distinct *gauge groups* which emerge from these string models (or equivalently, employing a different measure which assigns statistical weights to models according to the distinctness of their gauge groups), these results change somewhat:

- **88.55%** of our heterotic gauge groups contain $SO(2n \geq 6)$ factors; amongst these groups, the average number of such factors is ≈ 2.30 .
- **76.79%** of our heterotic gauge groups contain $SU(n \geq 3)$ factors; amongst these groups, the average number of such factors is ≈ 2.39 .
- **8.38%** of our heterotic gauge groups contain $E_{6,7,8}$ factors; amongst these groups, the average number of such factors is ≈ 1.06 .
- **97.62%** of our heterotic gauge groups contain $U(1)$ or $SU(2)$ factors; amongst these groups, the average number of such factors is ≈ 8.83 .

Note that the biggest relative change occurs for the exceptional groups, with over 8% of our gauge groups containing exceptional factors. Thus, we see that while exceptional gauge-group factors appear somewhat frequently within the set of allowed distinct heterotic gauge groups, the gauge groups containing exceptional factors emerge relatively rarely from our underlying heterotic string models.

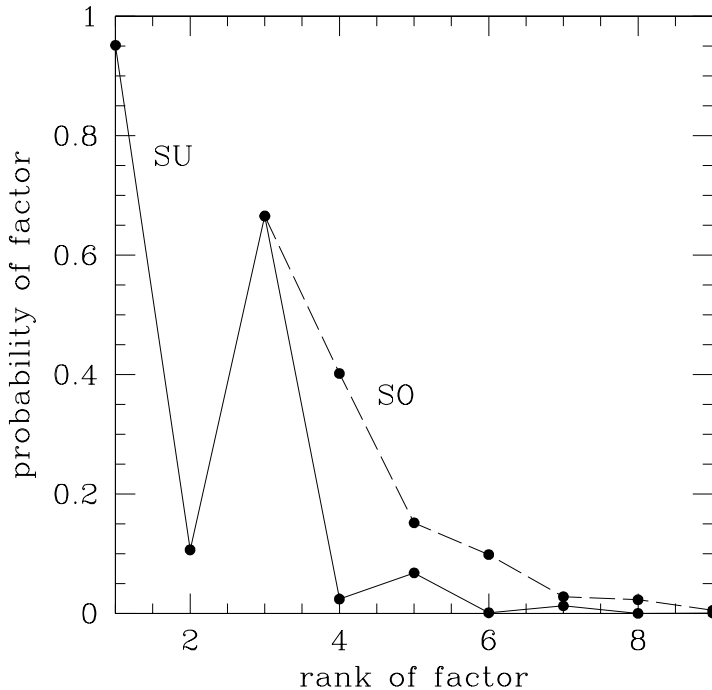


Figure 5: The probability that a given $SO(2n)$ or $SU(n+1)$ gauge-group factor appears at least once in the gauge group of a randomly chosen heterotic string model, plotted as a function of the rank n of the factor. While the ‘SU’ curve (solid line) is plotted for all ranks ≥ 1 , the ‘SO’ curve (dashed line) is only plotted for ranks ≥ 3 since $SO(2) \sim U(1)$ and $SO(4) \sim SU(2)^2$. These curves necessarily share a common point for rank 3, where $SU(4) \sim SO(6)$.

Of course, this information does not indicate the probabilities of individual ‘SO’ or ‘SU’ groups. Such individual probabilities are shown in Fig. 5, where we indicate the probabilities of individual ‘SO’ or ‘SU’ groups as functions of the ranks of these groups. We observe that for all ranks ≥ 3 , the ‘SU’ groups are significantly less common than the corresponding ‘SO’ groups. This pattern exists even for ranks up to 22, where the probabilities for ‘SU’ groups continue to be significantly less than those of their corresponding ‘SO’ counterparts. This helps to explain why, despite the information itemized above, the ‘SO’ groups are able to make a significantly larger contribution to the total rank than do the ‘SU’ groups, as illustrated in Fig. 4.

It is natural to wonder why the ‘SO’ groups tend to dominate over the ‘SU’ groups in this way, especially since ordinary quantum field theory would lead to no such preferences. Of course, it is entirely possible that these results may indicate some sort of bias in our sample of free-field string models. However, in a heterotic string framework, we recall that gauge symmetries ultimately have their origins as internal

symmetries amongst worldsheet fields. Indeed, within the free-field constructions we are examining, ‘SO’ groups tend to be the most natural since they represent rotational symmetries amongst identical worldsheet fields. By contrast, ‘SU’ groups are necessarily more difficult to construct, especially as the rank of the ‘SU’ group becomes relatively large.

We can illustrate this fact directly in the case of free-field worldsheet constructions by considering the relevant charge lattices for the gauge-boson states. These charges are nothing but the weights of the adjoint representations of these gauge groups, where each direction of the charge lattice corresponds to a different worldsheet field. It is then straightforward to consider how the different gauge groups are embedded in such a lattice, *i.e.*, how these gauge-boson states can be represented in terms of the underlying string degrees of freedom. For example, in a string formulation based upon complex worldsheet bosons ϕ_ℓ or fermions ψ_ℓ , each lattice direction \hat{e}_ℓ — and consequently each generator U_ℓ — corresponds to a different worldsheet boson or fermion: $U_\ell \equiv i\partial\phi_\ell = \overline{\psi}_\ell\psi_\ell$. Given such a construction, we simply need to understand how the simple roots of each gauge group are oriented with respect to these lattice directions.

Disregarding irrelevant overall lattice permutations and inversions, the ‘SO’ groups have a natural lattice embedding. For any group $SO(2n)$, the roots $\{\vec{\alpha}\}$ can be represented in an n -dimensional lattice as $\{\pm\hat{e}_i \pm \hat{e}_j\}$, with the simple roots given by $\vec{\alpha}_i = \hat{e}_i - \hat{e}_{i+1}$ for $1 \leq i \leq n-1$, and $\vec{\alpha}_n = \hat{e}_{n-1} + \hat{e}_n$. As we see, all coefficients for these embeddings are integers, which means that these charge vectors can be easily realized through excitations of Neveu-Schwarz worldsheet fermions.

By contrast, the group $SU(n)$ contains roots with necessarily non-integer coefficients if embedded in an $(n-1)$ -dimensional lattice [as appropriate for the rank of $SU(n)$]. For example, $SU(3)$ has two simple roots whose relative angle is $2\pi/3$, ensuring that no two-dimensional orthogonal coordinate system can be found with respect to which both roots have integer coordinates. In free-field string constructions, this problem is circumvented by embedding our $SU(n)$ groups into an n -dimensional lattice rather than an $(n-1)$ -dimensional lattice. One can then represent the $n-1$ simple roots as $\vec{\alpha}_i = \hat{e}_i - \hat{e}_{i+1}$ for $1 \leq i \leq n-1$, using only integer coefficients. However, this requires the use of an *extra* lattice direction in the construction — *i.e.*, this requires the coordinated participation of an additional worldsheet degree of freedom. Indeed, the $SU(n)$ groups are realized non-trivially only along diagonal hyperplanes within a higher-dimensional charge lattice. Such groups are consequently more difficult to achieve than their $SO(2n)$ cousins.

This also explains why the appearance of $SU(n)$ gauge groups is strongly correlated with the appearance of $U(1)$ factors in such free-field string models. As the above embedding indicates, in order to realize $SU(n)$ what we are really doing is first realizing $U(n) \equiv SU(n) \times U(1)$ in an n -dimensional lattice. In this n -dimensional lattice, the $U(1)$ group factor amounts to the trace of the $U(n)$ symmetry, and corresponds to the lattice direction $\vec{E} \equiv \sum_{\ell=1}^n \hat{e}_\ell$. The $(n-1)$ -dimensional hyperplane

orthogonal to \vec{E} then corresponds to the $SU(n)$ gauge group. Thus, in such free-field string models, we see that the appearance of $SU(n)$ gauge groups is naturally correlated with the appearance of $U(1)$ gauge groups. Indeed, within our statistical sample of heterotic string models, we find that

- **99.81% of all heterotic string models which contain one or more $SU(n)$ factors also exhibit an equal or greater number of $U(1)$ factors.** [In the remaining 0.19% of models, one or more of these $U(1)$ factors is absorbed to become part of another non-abelian group.] By contrast, the same can be said for only 74.62% of models with $SO(2n \geq 6)$ factors and only 61.07% of models with $E_{6,7,8}$ factors. Given that the average number of $U(1)$ factors per model across our entire statistical sample is ≈ 6.75 , these results for the ‘SO’ and ‘E’ groups are essentially random and do not reflect any underlying correlations.

Note that these last statements only apply to $SU(n)$ gauge-group factors with $n = 3$ or $n \geq 5$; the special case $SU(4)$ shares a root system with the orthogonal group $SO(6)$ and consequently does not require such an embedding.

For the purposes of realizing the Standard Model from heterotic strings, we may also be interested in the relative probabilities of achieving $SU(3)$, $SU(2)$, and $U(1)$ gauge-group factors individually. This information is shown in Fig. 6(a). Moreover, in Fig. 6(b), we show the joint probability of *simultaneously* obtaining at least one of each of these factors within a given string model, producing the combined factor $G_{\text{SM}} \equiv SU(3) \times SU(2) \times U(1)$. Indeed, averaging across all our heterotic string models, we find that

- **10.64%** of our heterotic string models contain $SU(3)$ factors; amongst these models, the average number of such factors is ≈ 1.88 .
- **95.06%** of our heterotic string models contain $SU(2)$ factors; amongst these models, the average number of such factors is ≈ 6.85 .
- **90.80%** of our heterotic string models contain $U(1)$ factors; amongst these models, the average number of such factors is ≈ 4.40 .

Note that these overall probabilities for $SU(3)$ and $SU(2)$ factors are consistent with those shown in Fig. 5. By contrast, across the set of allowed *gauge groups*, we find that

- **23.98%** of our heterotic gauge groups contain $SU(3)$ factors; amongst these groups, the average number of such factors is ≈ 2.05 .
- **73.87%** of our heterotic gauge groups contain $SU(2)$ factors; amongst these groups, the average number of such factors is ≈ 5.66 .
- **91.47%** of our heterotic gauge groups contain $U(1)$ factors; amongst these groups, the average number of such factors is ≈ 5.10 .

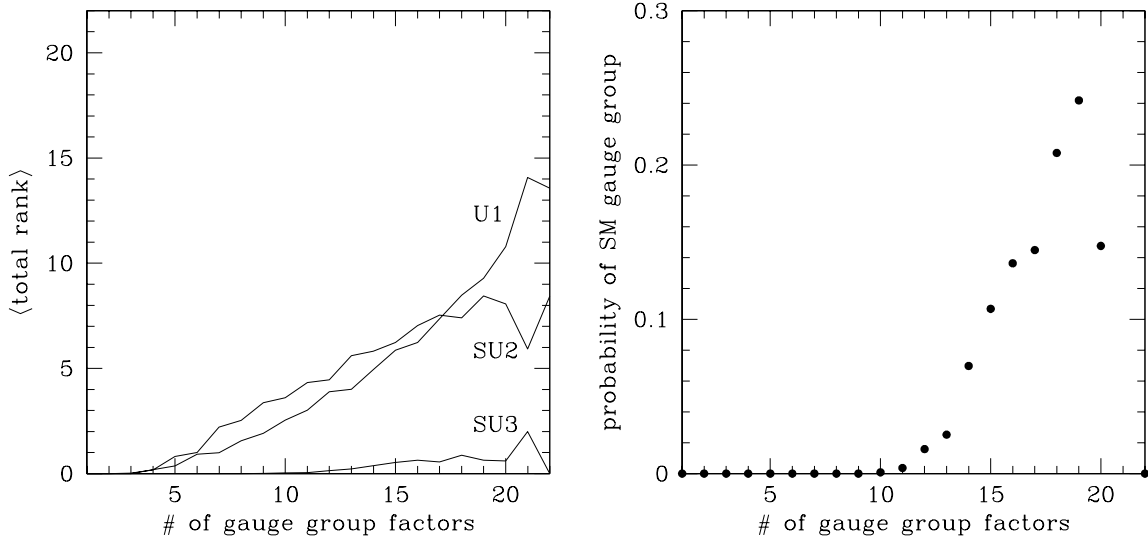


Figure 6: (a) (left) The distribution of total rank amongst $U(1)$, $SU(2)$, and $SU(3)$ gauge-group factors as a function of the total number of gauge-group factors. The sum of the $U(1)$ and $SU(2)$ lines reproduces the ‘I’ line in Fig. 4, while the $SU(3)$ line is a subset of the ‘SU’ line in Fig. 4. (b) (right) Absolute joint probability of obtaining a string model with the Standard-Model gauge group $G_{\text{SM}} \equiv SU(3) \times SU(2) \times U(1)$ as a function of the total number of gauge-group factors in the string model. Although off-scale and therefore not shown on this plot, the probability of realizing G_{SM} actually hits 1 for $f = 21$.

We see that the biggest relative change occurs for $SU(3)$ gauge-group factors: although such factors appear within almost 24% of the allowed gauge groups, these gauge groups emerge from underlying string models only half as frequently as we would have expected. This is why only 10% of our distinct heterotic string models contain $SU(3)$ gauge-group factors.

At first glance, it may seem that these results for $SU(2)$ and $U(1)$ factors conflict with the results in Fig. 6(a). However, the total number of models containing at least one gauge-group factor of a given type is dependent not only on the average rank contributed by a given class of gauge group as a function of f [as shown in Fig. 6(a)], but also on the overall number of models as a function of f [as shown in Fig. 1]. Thus, these plots provide independent information corresponding to different ways of correlating and presenting statistics for the same data set.

As we see from Fig. 6(a), $SU(3)$ gauge factors do not statistically appear in our heterotic string models until the overall gauge group has been “shattered” into at least eight irreducible factors. Moreover, as we have seen, the net probabilities of $SU(2)$ and $U(1)$ factors peak only when there are relatively large numbers of factors. Consequently, we observe from the joint probabilities in Fig. 6(b) that the entire Standard-Model gauge group does not statistically appear until our overall gauge

group has been shattered into at least 10 gauge-group factors. This precludes the appearance of gauge groups such as $G_{\text{SM}} \times SO(36)$, $G_{\text{SM}} \times E_6 \times SO(24)$, and so forth — all of which would have been allowed on the basis of rank and central charge constraints. Once again, it is the constraint of the self-duality of the complete charge lattice — *i.e.*, the modular invariance of the underlying string model — which is ultimately the origin of such correlations. These results also agree with what has been found in several explicit (supersymmetric) semi-realistic perturbative heterotic string models with Standard-Model gauge groups [27].

Note from Fig. 6(b) that the probability of obtaining the Standard-Model gauge group actually hits 100% for $f = 21$, and drops to zero for $f = 22$. Both features are easy to explain in terms of correlations we have already seen. For $f = 21$, our gauge groups are *required* to contain an $SU(3)$ factor since there are no simply-laced irreducible rank-two groups other than $SU(3)$. [This is also why the $SU(3)$ factors always contribute exactly two units of rank to the overall rank for $f = 21$, as indicated in Fig. 6(a).] For $f = 22$, by contrast, no $SU(3)$ factors can possibly appear.

Another important issue for string model-building concerns cross-correlations between *different* gauge groups — *i.e.*, the joint probabilities that two different gauge groups appear simultaneously within a single heterotic string model. For example, while one gauge-group factor may correspond to our observable sector, the other factor may correspond to a hidden sector. Likewise, for model-building purposes, we might also be interested in probabilities that involve the entire Standard-Model gauge group $G_{\text{SM}} \equiv SU(3) \times SU(2) \times U(1)$ or the entire Pati-Salam gauge group $G_{\text{PS}} \equiv SU(4) \times SU(2)^2$.

This information is collected in Table 1. It is easy to read a wealth of information from this table. For example, this table provides further confirmation of our previous claim that nearly all heterotic string models which contain an $SU(n \geq 3)$ factor for $n \neq 4$ also contain a corresponding $U(1)$ factor. [Recall that $SU(4)$ is a special case: since $SU(4) \sim SO(6)$, the roots of $SU(4)$ have integer coordinates in a standard lattice embedding.]

Likewise, we see from this table that

- **The total probability of obtaining the Standard-Model gauge group across our entire sample set is only 10.05%, regardless of what other gauge-group factors are present.**

This is similar to what is found for Type I strings [5], and agrees with the sum of the data points shown in Fig. 6(b) after they are weighted by the results shown in Fig. 1. Since we have seen that only 10.64% of our heterotic string models contain at least one $SU(3)$ gauge factor [as compared with 95.06% for $SU(2)$ and 90.80% for $U(1)$], we conclude that *the relative scarcity of $SU(3)$ factors is the dominant feature involved in suppressing the net probability of appearance of the Standard-Model gauge group*. Indeed, the relative scarcity of $SU(3)$ gauge-group factors is amply illustrated in this table.

	U_1	SU_2	SU_3	SU_4	SU_5	$SU_{>5}$	SO_8	SO_{10}	$SO_{>10}$	$E_{6,7,8}$	SM	PS
U_1	87.13	86.56	10.64	65.83	2.41	8.20	32.17	14.72	8.90	0.35	10.05	61.48
SU_2		94.05	10.05	62.80	2.14	7.75	37.29	13.33	12.80	0.47	9.81	54.31
SU_3			7.75	5.61	0.89	0.28	1.44	0.35	0.06	10^{-5}	7.19	5.04
SU_4				35.94	1.43	5.82	24.41	11.15	6.53	0.22	5.18	33.29
SU_5					0.28	0.09	0.46	0.14	0.02	0	0.73	1.21
$SU_{>5}$						0.59	3.30	1.65	1.03	0.06	0.25	4.87
SO_8							12.68	6.43	8.66	0.30	1.19	22.02
SO_{10}								2.04	2.57	0.13	0.25	9.44
$SO_{>10}$									3.03	0.25	0.03	5.25
$E_{6,7,8}$										0.01	0	0.13
SM											7.12	3.86
PS												26.86
total:	90.80	95.06	10.64	66.53	2.41	8.20	40.17	15.17	14.94	0.57	10.05	62.05

Table 1: Percentages of four-dimensional heterotic string models which exhibit various combinations of gauge groups. Columns/rows labeled as $SU_{>5}$, $SO_{>10}$, and $E_{6,7,8}$ indicate *any* gauge group in those respective categories [e.g., $SU_{>5}$ indicates any gauge group $SU(n)$ with $n > 5$]. Off-diagonal entries show the percentage of models whose gauge groups simultaneously contain the factors associated with the corresponding rows/columns, while diagonal entries show the percentage of models which meet the corresponding criteria at least *twice*. For example, 7.75% of models contain an $SU(2) \times SU(n)$ factor with any $n > 5$, while 35.94% of models contain at least two $SU(4)$ factors. ‘SM’ and ‘PS’ respectively indicate the Standard-Model gauge group $G_{\text{SM}} \equiv SU(3) \times SU(2) \times U(1)$ and the Pati-Salam gauge group $G_{\text{PS}} \equiv SU(4) \times SU(2)^2$. Thus, only 0.13% of models contain G_{PS} together with an exceptional group, while 33.29% of models contain at least $G_{\text{PS}} \times SU(2) = SU(4)^2 \times SU(2)^2$ and 26.86% of models contain at least $G_{\text{PS}}^2 = SU(4)^2 \times SU(2)^4$. A zero entry indicates that no string model with the required properties was found, whereas the entry 10^{-5} indicates the existence of a single string model with the given properties. Entries along the ‘total’ row indicate the total percentages of models which have the corresponding gauge-group factor, regardless of what other gauge groups may appear; note that this is *not* merely the sum of the joint probabilities along a row/column since these joint probabilities are generally not exclusive. For example, although 86.56% of models have both an $SU(2)$ factor and a $U(1)$ factor and 94.05% of models contain $SU(2)^2$, the total percentage of models containing an $SU(2)$ factor is only slightly higher at 95.06%, as claimed earlier. Note that nearly every string model which contains an $SU(n \geq 3)$ gauge-group factor for $n \neq 4$ also contains a $U(1)$ gauge-group factor, as discussed earlier; thus, the joint and individual probabilities are essentially equal in this case. Also note that only 10.05% of heterotic string models contain the Standard-Model gauge group, regardless of other correlations; moreover, when this gauge group appears, it almost always comes with an additional $SU(2)$, $SU(3)$, or $SU(4)$ factor.

It is also apparent that among the most popular GUT groups $SU(5)$, $SO(10)$, and E_6 , the choice $SO(10)$ is most often realized across this sample set. This again reflects the relative difficulty of realizing ‘SU’ and ‘E’ groups. Indeed,

- **The total probability of obtaining a potential GUT group of the form $SO(2n \geq 10)$ across our entire sample set is 24.5%, regardless of what other gauge-group factors are present. For $SU(n \geq 5)$ and $E_{6,7,8}$ GUT groups, by contrast, these probabilities fall to 7.7% and 0.2% respectively.**

Once again, we point out that these numbers are independent of those in Table 1, since the sets of models exhibiting $SO(10)$ versus $SO(2n > 10)$ factors [or exhibiting $SU(5)$ versus $SU(n > 5)$ factors] are not mutually exclusive.

Note that for the purposes of this tally, we are considering the $SO(4n \geq 12)$ groups as potential GUT groups even though they do not have complex representations; after all, these groups may dynamically break at lower energies to the smaller $SO(4n - 2 \geq 10)$ groups which do. Moreover, although we are referring to such groups as “GUT” groups, we do not mean to imply that string models realizing these groups are necessarily suitable candidates for realizing various grand-unification scenarios. We only mean to indicate that these gauge groups are those that are found to have unification possibilities in terms of the quantum numbers of their irreducible representations. In order for a string model to realize a complete unification scenario, it must also give rise to the GUT Higgs field which is necessary for breaking the GUT group down to that of the Standard Model. For each of the potential GUT groups we are discussing, the smallest Higgs field that can accomplish this breaking must transform in the adjoint representation of the GUT group, and string unitarity constraints imply that such Higgs fields cannot appear in the massless string spectrum unless these GUT groups are realized at affine level $k > 1$. This can only occur in models which also exhibit rank-cutting [28, 29], and as discussed in Sect. 2, this is beyond the class of models we are examining. Nevertheless, there are many ways in which such models may incorporate alternative unification scenarios. For example, such GUT groups may be broken by field-theoretic means (*e.g.*, through effective or composite Higgs fields which emerge by running to lower energies and which therefore do not correspond to elementary string states at the string scale).

Thus far, we have paid close attention to the *ranks* of the gauge groups. There is, however, another important property of these groups, namely their *orders* or dimensions (*i.e.*, the number of gauge bosons in the massless spectrum of the corresponding string model). This will be particularly relevant in Sect. 6 when we examine correlations between gauge groups and one-loop vacuum amplitudes (cosmological constants).

Although we find 1301 gauge groups for our $\sim 10^5$ models, it turns out that these gauge groups have only 95 distinct orders. These stretch all the way from 22 [for $U(1)^{22}$] to 946 [for $SO(44)$]. Note that the 22 gauge bosons for $U(1)^{22}$ are nothing

but the Cartan generators at the origin of our 22-dimensional charge lattice, with all higher orders signalling the appearance of additional non-Cartan generators which enhance these generators to form larger, non-abelian Lie groups.

In Fig. 7(a), we show the average orders of our string gauge groups as a function of the number f of gauge-group factors, where the average is calculated over all string models sharing a fixed f . Within the set of models with fixed f , the orders of the corresponding gauge groups can vary wildly. However, the average exhibits a relatively smooth behavior, as seen in Fig. 7(a).

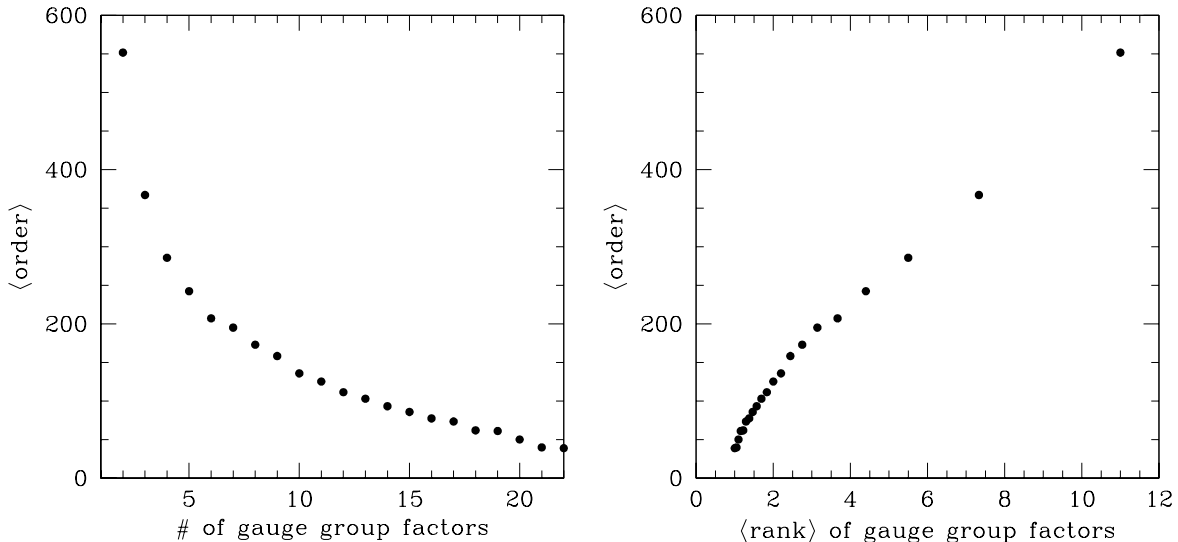


Figure 7: (a) (left) The orders (dimensions) of the gauge groups (*i.e.*, the number of gauge bosons) averaged over all heterotic string models with a fixed number f of gauge-group factors, plotted as a function of f . The monotonic shape of this curve indicates that on average — and despite the contributions from twisted sectors — the net effect of breaking gauge groups into smaller irreducible factors is to project non-Cartan gauge bosons out of the massless string spectrum. The $f = 1$ point with order 946 is off-scale and hence not shown. (b) (right) Same data, plotted versus the average rank per gauge group factor in such models, defined as $22/f$. On this plot, the extra point for $f = 1$ with order 946 would correspond to $\langle \text{rank} \rangle = 22$ and thus continues the asymptotically linear behavior.

It is easy to understand the shape of this curve. Ordinarily, we expect the order of a Lie gauge-group factor to scale as the square of its rank r :

$$\text{order} \sim pr^2 \quad \text{for } r \gg 1 \quad (4.1)$$

where the proportionality constant for large r is

$$p = \begin{cases} 1 & \text{for } SU(r+1) \\ 2 & \text{for } SO(2r) \\ \approx 2.17 & \text{for } E_6 \\ \approx 2.71 & \text{for } E_7 \\ \approx 3.88 & \text{for } E_8 . \end{cases} \quad (4.2)$$

(For the E groups, these values of p are merely the corresponding orders divided by the corresponding ranks.) Thus, for the total gauge group of a given string model, we expect the total order to scale as

$$\text{order} \sim \langle p \rangle \cdot \langle r^2 \rangle \cdot \langle \# \text{ of factors} \rangle \quad (4.3)$$

However, letting $f = \langle \# \text{ of factors} \rangle$, we see that for our heterotic string models, $\langle r \rangle = 22/f$. We thus find that

$$\text{order} \sim (22)^2 \langle p \rangle \frac{1}{\langle \# \text{ of factors} \rangle} \sim 22 \langle p \rangle \langle \text{rank} \rangle \quad (4.4)$$

where we are neglecting all terms which are subleading in the average rank.

In Fig. 7(b), we have plotted the same data as in Fig. 7(a), but as a function of $\langle \text{rank} \rangle \equiv 22/f$. We see that our expectations of roughly linear behavior are indeed realized for large values of $\langle \text{rank} \rangle$, with an approximate numerical value for $\langle p \rangle$ very close to 2. Given Eq. (4.2), this value for $\langle p \rangle$ reflects the dominance of the ‘SO’ groups, with the contributions from ‘SU’ groups tending to cancel the contributions of the larger but rarer ‘E’ groups. For smaller values of $\langle \text{rank} \rangle$, however, we observe a definite curvature to the plot in Fig. 7(b). This reflects the contributions of the subleading terms that we have omitted from Eq. (4.1) and from our implicit identification of $\langle r^2 \rangle \sim \langle r \rangle^2$ in passing from Eq. (4.3) to Eq. (4.4).

Fig. 7(a) demonstrates that as we “shatter” our gauge groups (*e.g.*, through orbifold twists), the net effect is to project non-Cartan gauge bosons out of the string spectrum. While this is to be expected, we emphasize that this need not always happen in a string context. Because of the constraints coming from modular invariance and anomaly cancellation, performing an orbifold projection in one sector requires that we introduce a corresponding “twisted” sector which can potentially give rise to new non-Cartan gauge bosons that replace the previous ones. The most famous example of this phenomenon occurs in ten dimensions: starting from the supersymmetric $SO(32)$ heterotic string (with 496 gauge bosons), we might attempt an orbifold twist to project down to the gauge group $SO(16) \times SO(16)$ (which would have had only 240 gauge bosons). However, if we also wish to preserve spacetime supersymmetry, we are forced to introduce a twisted sector which provides exactly 256 extra gauge bosons to replace those that were lost, thereby enhancing the resulting $SO(16) \times SO(16)$ gauge group back up to $E_8 \times E_8$ (which again has 496 gauge

bosons). As evident from Fig. 7(a), there are several places on the curve at which increasing the number of gauge-group factors by one unit does not appear to significantly decrease the average order; indeed, this phenomenon of extra gauge bosons emerging from twisted sectors is extremely common across our entire set of heterotic string models. However, we see from Fig. 7(a) that *on average*, more gauge-group factors implies a diminished order, as anticipated in Eq. (4.4).

For later purposes, it will also be useful for us to evaluate the “inverse” map which gives the average number of gauge-group factors as function of the total order. Since our models give rise to 95 distinct orders, it is more effective to provide this map in the form of a histogram. The result is shown in Fig. 8. Note that because this “inverse” function is binned according to orders rather than averaged ranks, models are distributed differently across the data set and thus Fig. 8 actually contains independent information relative to Fig. 7. However, the shape of the resulting curve in Fig. 8 is indeed independent of bin *size*, as necessary for statistical significance.

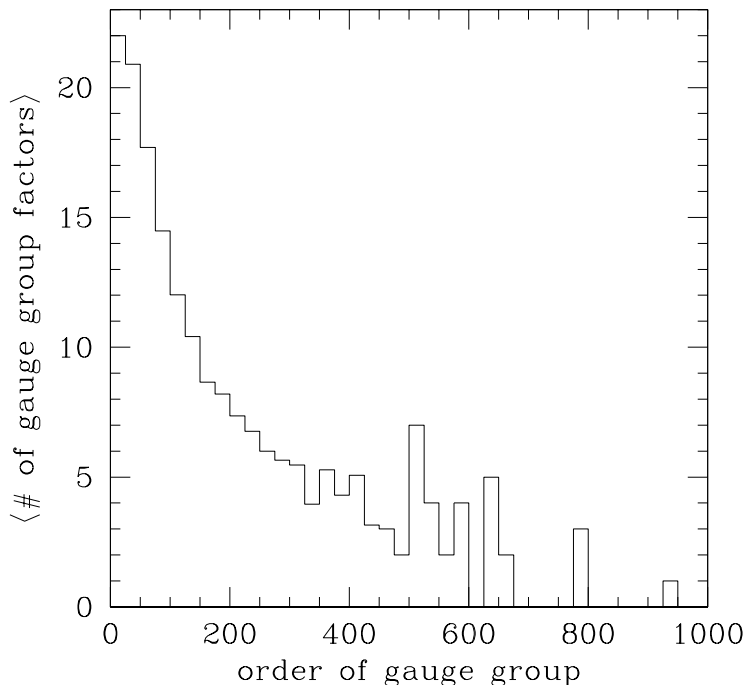


Figure 8: Histogram illustrating the “inverse” of Fig. 7. This plot shows the number of gauge-group factors, averaged over all heterotic string models with a given gauge-group order (dimension).

Once again, many of the features in Fig. 8 can be directly traced back to the properties of our original model “tree”. At the right end of the histogram, for example, we see the contribution from the $SO(44)$ model (for which $f = 1$), with order

946. This is the model with the highest order. After this, with order 786, are two models with gauge group $SO(40) \times SU(2)^2$, followed by 12 models with gauge group $SO(36) \times SO(8)$ at order 658. This is why the histogram respectively shows exactly $\langle f \rangle = 3$ and $\langle f \rangle = 2$ at these orders. This pattern continues as the orders descend, except that we start having multiple gauge groups contributing with the same order. For example, at order 466, there are twelve models with three distinct rank-22 simply-laced gauge groups: five models with gauge group $SO(24) \times SO(20)$, two models with gauge group $E_8 \times SO(20) \times SO(8)$, and five models with gauge group $SO(30) \times SU(4)^2 \times U(1)$. Combined, this yields $\langle f \rangle = 3$, as shown in Fig. 8 for order 466. Finally, at the extreme left edge of Fig. 8, we see the contributions from models with $f = 22$, which necessarily have orders ≤ 66 .

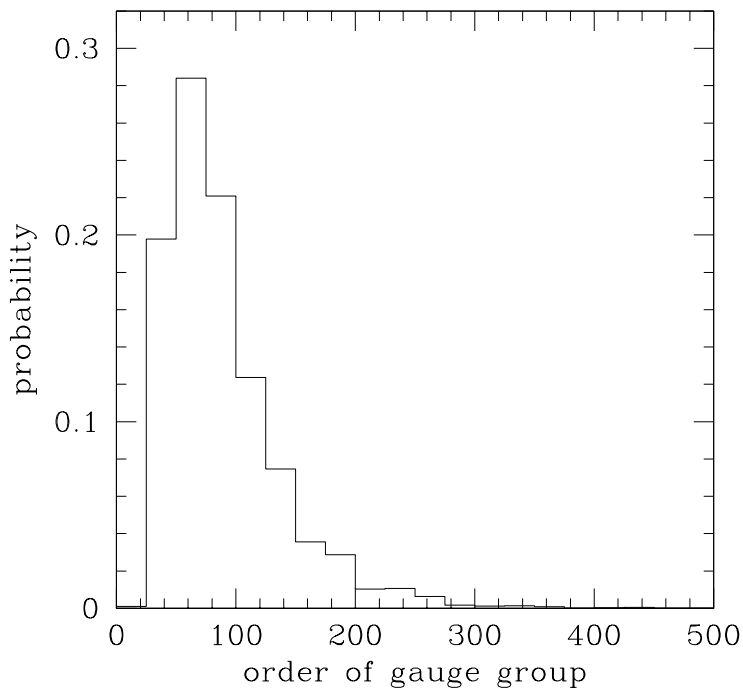


Figure 9: Histogram illustrating the absolute probabilities of obtaining distinct four-dimensional heterotic string models as a function of the orders of their gauge groups. The total probability from all bins (the “area under the curve”) is 1, with models having orders exceeding 300 relatively rare.

We can also plot the absolute probabilities of obtaining distinct four-dimensional string models as a function of the orders of their gauge groups. This would be the analogue of Fig. 1, but with probabilities distributed as functions of orders rather than numbers of gauge-group factors. The result is shown in Fig. 9. As we see from Fig. 9, models having orders exceeding 200 are relatively rare.

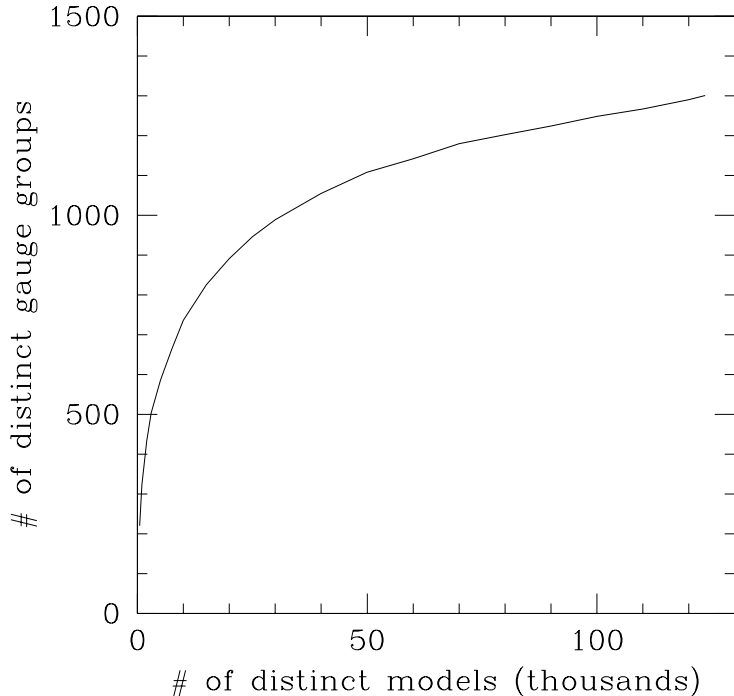


Figure 10: The number of gauge groups obtained as a function of the number of distinct heterotic string models examined. While the total number of models examined is insufficient to calculate a precise shape for this curve, one possibility is that this curve will eventually saturate at a maximum number of possible gauge groups.

As a final topic, we have already noticed that our data set of $\gtrsim 10^5$ distinct models has yielded only 1301 different gauge groups. There is, therefore, a huge redundancy of gauge groups as far as our models are concerned, with it becoming increasingly difficult to find new heterotic string models exhibiting gauge groups which have not been seen before. In Fig. 10, we show the number of gauge groups that we obtained as a function of the number of distinct heterotic string models we examined. Clearly, although the total number of models examined is insufficient to calculate a precise shape for this curve, one possibility is that this curve will eventually saturate at a maximum number of possible gauge groups which is relatively small. This illustrates the tightness of the modular-invariance constraints in restricting the set of possible allowed gauge groups.

5 Cosmological constants: Statistical results

We now turn to calculations of the vacuum energy densities (or cosmological constants) corresponding to these heterotic string vacua. Since the tree-level contri-

butions to these cosmological constants all vanish as a result of conformal invariance, we shall focus exclusively on their one-loop contributions. These one-loop cosmological constants λ may be expressed in terms of the one-loop zero-point functions Λ , defined as

$$\Lambda \equiv \int_{\mathcal{F}} \frac{d^2\tau}{(\text{Im } \tau)^2} Z(\tau). \quad (5.1)$$

Here $Z(\tau)$ is the one-loop partition function of the tree-level string spectrum of the model in question (after GSO projections have been implemented); $\tau \equiv \tau_1 + i\tau_2$ is the one-loop toroidal complex parameter, with $\tau_i \in \mathbb{R}$; and $\mathcal{F} \equiv \{\tau : |\text{Re } \tau| \leq \frac{1}{2}, \text{Im } \tau > 0, |\tau| \geq 1\}$ is the fundamental domain of the modular group. Because the string models under consideration are non-supersymmetric but tachyon-free, Λ is guaranteed to be finite and in principle non-zero. The corresponding one-loop vacuum energy density (cosmological constant) λ is then defined as $\lambda \equiv -\frac{1}{2}\mathcal{M}^4\Lambda$, where $\mathcal{M} \equiv M_{\text{string}}/(2\pi)$ is the reduced string scale. Although Λ and λ have opposite signs, with Λ being dimensionless, we shall occasionally refer to Λ as the cosmological constant in cases where the overall sign of Λ is not important.

Of course, just as with the ten-dimensional $SO(16) \times SO(16)$ string, the presence of a non-zero Λ indicates that these string models are unstable beyond tree level. Thus, as discussed in the Introduction, these vacua are generically not situated at local minima within our “landscape”, and can be expected to become unstable as the string coupling is turned on. Nevertheless, we shall investigate the values of these amplitudes for a number of reasons. First, the amplitude defined in Eq. (5.1) represents possibly the simplest one-loop amplitude that can be calculated for such models; as such, it represents a generic quantity whose behavior might hold lessons for more complicated amplitudes. For example, more general n -point amplitudes are related to this amplitude through differentiations; a well-known example of this is provided by string threshold corrections [30], which are described by a similar modular integration with a slightly altered (differentiated) integrand. Second, by evaluating and analyzing such string-theoretic expressions, we can gain insight into the extent to which results from effective supergravity calculations might hold in a full string context. Indeed, we shall be able to judge exactly how significant a role the massive string states might play in altering our field-theoretic expectations based on considerations of only the massless states. Third, when we eventually combine this information with our gauge-group statistics in Sect. 6, we shall be able to determine the extent to which gauge groups and the magnitudes of such scattering amplitudes might be correlated in string theory. But finally and most importantly, we shall investigate this amplitude because it relates directly back to fundamental questions of supersymmetry breaking and vacuum stability. Indeed, if we can find models for which Λ is nearly zero, we will have found good approximations to stable vacua with broken supersymmetry. We shall also discover other interesting features, such as unexpected one-loop degeneracies in the space of non-supersymmetric string models. All of this may represent important information concerning the properties of the

landscape of *non*-supersymmetric strings.

In general, the one-loop partition function $Z(\tau)$ which appears in Eq. (5.1) is defined as the trace over the full Fock space of string states:

$$Z(\tau) \equiv \text{Tr}(-1)^F \bar{q}^{H_R} q^{H_L} . \quad (5.2)$$

Here F is the spacetime fermion number, (H_R, H_L) are the right- and left-moving worldsheet Hamiltonians, and $q \equiv \exp(2\pi i\tau)$. Thus spacetime bosonic states contribute positively to $Z(\tau)$, while fermionic states contribute negatively. In general, the trace in Eq. (5.2) may be evaluated in terms of the characters χ_i and $\bar{\chi}_j$ of the left- and right-moving conformal field theories on the string worldsheet,

$$Z(\tau) = \tau_2^{-1} \sum_{i,j} \bar{\chi}_j(\bar{\tau}) N_{ji} \chi_i(\tau) , \quad (5.3)$$

where the coefficients N_{ij} describe the manner in which the left- and right-moving CFT's are stitched together and thereby reflect the particular GSO projections inherent in the given string model. The τ_2^{-1} prefactor in Eq. (5.3) represents the contribution to the trace in Eq. (5.2) from the continuous spectrum of states corresponding to the uncompactified spacetime dimensions.

Since the partition function $Z(\tau)$ represents a trace over the string Fock space as in Eq. (5.2), it encodes the information about the net degeneracies of string states at each mass level in the theory. Specifically, expanding $Z(\tau)$ as a double-power series in (q, \bar{q}) , we obtain an expression of the form

$$Z(\tau) = \tau_2^{-1} \sum_{mn} b_{mn} \bar{q}^m q^n \quad (5.4)$$

where (m, n) represent the possible eigenvalues of the right- and left-moving worldsheet Hamiltonians (H_R, H_L) , and where b_{mn} represents the net number of bosonic minus fermionic states (spacetime degrees of freedom) which actually have those eigenvalues and satisfy the GSO constraints. Modular invariance requires that $m - n \in \mathbb{Z}$ for all $b_{mn} \neq 0$; a state is said to be “on-shell” or “level-matched” if $m = n$, and corresponds to a spacetime state with mass $\mathcal{M}_n = 2\sqrt{n}M_{\text{string}}$. Thus, states for which $m + n \geq 0$ are massive and/or massless, while states with $m + n < 0$ are tachyonic. By contrast, states with $m - n \in \mathbb{Z} \neq 0$ are considered to be “off-shell”: they contribute to one-loop amplitudes such as Λ with a dependence on $|m - n|$, but do not correspond to physical states in spacetime.

Substituting Eq. (5.4) into Eq. (5.1), we have

$$\begin{aligned} \Lambda &= \sum_{m,n} b_{mn} \int_{\mathcal{F}} \frac{d^2\tau}{\tau_2^2} \tau_2^{-1} \bar{q}^m q^n \\ &= \sum_{m,n} b_{mn} \int_{\mathcal{F}} \frac{d^2\tau}{\tau_2^3} \exp[-2\pi(m+n)\tau_2] \cos[2\pi(m-n)\tau_1] . \end{aligned} \quad (5.5)$$

(Note that since \mathcal{F} is symmetric under $\tau_1 \rightarrow -\tau_1$, only the cosine term survives in passing to the second line.) Thus, we see that the contributions from different regions of \mathcal{F} will depend critically on the values of m and n . The contribution to Λ from the $\tau_2 < 1$ region is always finite and non-zero for all values of m and n . However, given that $m - n \in \mathbb{Z}$, we see that the contribution from the $\tau_2 > 1$ region is zero if $m \neq n$, non-zero and finite if $m = n > 0$, and infinite if $m = n < 0$.

For heterotic strings, our worldsheet vacuum energies are bounded by $m \geq -1/2$ and $n \geq -1$. Moreover, all of the models we are considering in this paper are tachyon-free, with $b_{mn} = 0$ for all $m = n < 0$. As a result, in such models, each contribution to Λ is finite and non-zero. By contrast, note that a supersymmetric string model would have $b_{mn} = 0$ for all (m, n) , leading to $\Lambda = 0$. Non-zero values of Λ are thus a signature for broken spacetime supersymmetry.

For simplicity, we can change variables from (m, n) to $(s \equiv m + n, d \equiv |n - m|)$. Indeed, since $\Lambda \in \mathbb{R}$, we can always take $d \geq 0$ and define

$$a_{sd} \equiv b_{(s-d)/2, (s+d)/2} + b_{(s+d)/2, (s-d)/2} . \quad (5.6)$$

We can thus rewrite Eq. (5.5) in the form

$$\Lambda = \sum_{s,d} a_{sd} I_{sd} \quad \text{where} \quad I_{sd} \equiv \int_{\mathcal{F}} \frac{d^2\tau}{\tau_2^3} \exp(-2\pi s\tau_2) \cos(2\pi d\tau_1) . \quad (5.7)$$

For heterotic strings, this summation is over all $s \geq -1$ and $|d| = 0, 1, \dots, [s] + 2$ where $[x]$ signifies the greatest integer $\leq x$. Of course, only those states with $d = 0$ are on-shell, but Λ receives contributions from off-shell states with non-zero d as well. In general, the values of s which appear in a given string model depend on a number of factors, most notably the conformal dimensions of the worldsheet fields (which in turn depend on various internal compactification radii); however, for the class of models considered in this paper, we have $s \in \mathbb{Z}/2$. The numerical values of I_{sd} from the lowest-lying string states with $s \leq 1.5$ are listed in Table 2.

We immediately observe several important features. First, although the coefficients a_{sd} tend to experience an exponential (Hagedorn) growth $a_{sd} \sim e^{\sqrt{s}}$, we see that the values of I_{sd} generally decrease exponentially with s , *i.e.*, $I_{sd} \sim e^{-s}$. This is then sufficient to overcome the Hagedorn growth in the numbers of states, leading to a convergent value of Λ . However, because of the balancing between these two effects, it is generally necessary to determine the complete particle spectrum of each vacuum state up to a relatively high (*e.g.*, fifth or sixth) mass level, with $s \approx 5$ or 6 , in order to accurately calculate the full cosmological constant Λ for each string model. This has been done for all results quoted below.

Second, we observe that the contributions $I_{s,0}$ from all on-shell states are positive, *i.e.*, $I_{s,0} > 0$ for all s . Thus, as anticipated on field-theoretic grounds, on-shell bosonic states contribute positively to Λ , while on-shell fermionic states contribute negatively. (Note that this is reversed for the actual cosmological constant λ , which differs from

s	d	I_{sd}	s	d	I_{sd}
-1.0	1	-12.192319	1.0	0	0.000330
-0.5	1	-0.617138	1.0	1	-0.000085
0.0	0	0.549306	1.0	2	0.000035
0.0	1	-0.031524	1.0	3	-0.000018
0.0	2	0.009896	1.5	0	0.000013
0.5	0	0.009997	1.5	1	-0.000004
0.5	1	-0.001626	1.5	2	0.000002
0.5	2	0.000587	1.5	3	-0.000001

Table 2: Contributions to the one-loop string vacuum amplitude I_{sd} defined in Eq. (5.7) from the lowest-lying string states with $s \leq 1.5$.

Λ by an overall sign.) However, we more generally observe that $I_{sd} > 0$ (< 0) for even (odd) d . Thus, the first group of off-shell states with $d = 1$ tend to contribute oppositely to the corresponding on-shell states with $d = 0$, with this behavior partially compensated by the second group of off-shell states with $d = 2$, and so forth. This, along with the fact [31] that the coefficients a_{sd} necessarily exhibit a regular oscillation in their overall signs as a function of s , also aids in the convergence properties of Λ .

Finally, we observe that by far the single largest contributions to the vacuum amplitude Λ actually come from states with $(s, d) = (-1, 1)$, or $(m, n) = (0, -1)$. These states are off-shell tachyons. At first glance one might suspect that it would be possible to project such states out of the spectrum (just as one does with the on-shell tachyons), but it turns out that this is impossible: *all heterotic string models necessarily have off-shell tachyons with $(m, n) = (0, -1)$* . These are “proto-graviton” states emerging in the Neveu-Schwarz sector:

$$\text{proto-graviton:} \quad \tilde{b}_{-1/2}^\mu |0\rangle_R \otimes |0\rangle_L \quad (5.8)$$

where $\tilde{b}_{-1/2}^\mu$ represents the excitation of the right-moving worldsheet Neveu-Schwarz fermion $\tilde{\psi}^\mu$. Since the Neveu-Schwarz heterotic string ground state has vacuum energies $(H_R, H_L) = (-1/2, -1)$, we see that the “proto-graviton” state in Eq. (5.8) has worldsheet energies $(H_R, H_L) = (m, n) = (0, -1)$; indeed, this is nothing but the graviton state without its left-moving oscillator excitation. However, note that regardless of the particular GSO projections, the graviton state must always appear in the string spectrum. Since GSO projections are insensitive to the oscillator excitations, this implies that the proto-graviton must also necessarily appear in the string spectrum.

By itself, of course, this argument does not prove that we must necessarily have $a_{-1,1} \neq 0$. However, it is easy to see that the only state which could possibly cancel the contribution from the (bosonic) proto-graviton in the Neveu-Schwarz sector is a

(fermionic) proto-gravitino in the Ramond sector:

$$\text{proto-gravitino:} \quad \{\tilde{b}_0\}^\alpha |0\rangle_R \otimes |0\rangle_L . \quad (5.9)$$

Here $\{\tilde{b}_0\}^\alpha$ schematically indicates the Ramond zero-mode combinations which collectively give rise to the spacetime Lorentz spinor index α . However, if the gravitino itself is projected out of the spectrum (producing the non-supersymmetric string model), then that same GSO projection must simultaneously project out the proto-gravitino state. In other words, while all heterotic strings contain a proto-graviton state, only those with spacetime supersymmetry will contain a compensating proto-gravitino state. Thus, all non-supersymmetric heterotic string models must have an uncancelled $a_{-1,1} > 0$.

This fact has important implications for the overall sign of Λ . *A priori*, we might have expected that whether Λ is positive or negative would be decided primarily by the net numbers of massless, on-shell bosonic and fermionic states in the string model — *i.e.*, by the sign of a_{00} . However, we now see that because $a_{-1,1} > 0$ and $I_{-1,1} < 0$, there is already a built-in bias towards negative values of Λ for heterotic strings. Indeed, each off-shell tachyon can be viewed as providing an initial negative offset for Λ of magnitude $I_{-1,1} \approx -12.19$, so that there is an approximate critical value for a_{00} , given by

$$a_{00} \Big|_{\text{critical}} \approx -\frac{I_{-1,1}}{I_{0,0}} \approx 22.2 , \quad (5.10)$$

which is needed just to balance each off-shell tachyon and obtain a vanishing Λ . Of course, even this estimate is low, as it ignores the contributions of off-shell *massless* states which, like the off-shell tachyon, again provide negative contributions for bosons and positive contributions for fermions.

The lesson from this discussion, then, is clear:

- **In string theory, contributions from the infinite towers of string states, both on-shell and off-shell, are critical for determining not only the magnitude but also the overall sign of the one-loop cosmological constant.** Examination of the massless string spectrum (*e.g.*, through a low-energy effective field-theory analysis) is insufficient.

We now turn to the values of Λ that are obtained across our set of heterotic string models. For each model, we evaluated the on- and off-shell degeneracies a_{sd} to at least the fifth level ($s \approx 5$), and then tabulated the corresponding value of Λ as in Eq. (5.7). A histogram illustrating the resulting distribution of cosmological constants is shown in Fig. 11.

As can be seen, both positive and negative values of Λ are obtained, and indeed the bulk of these models have values of Λ centered near zero. In fact, despite the contributions of the off-shell tachyons, it is evident from Fig. 11 that there is a

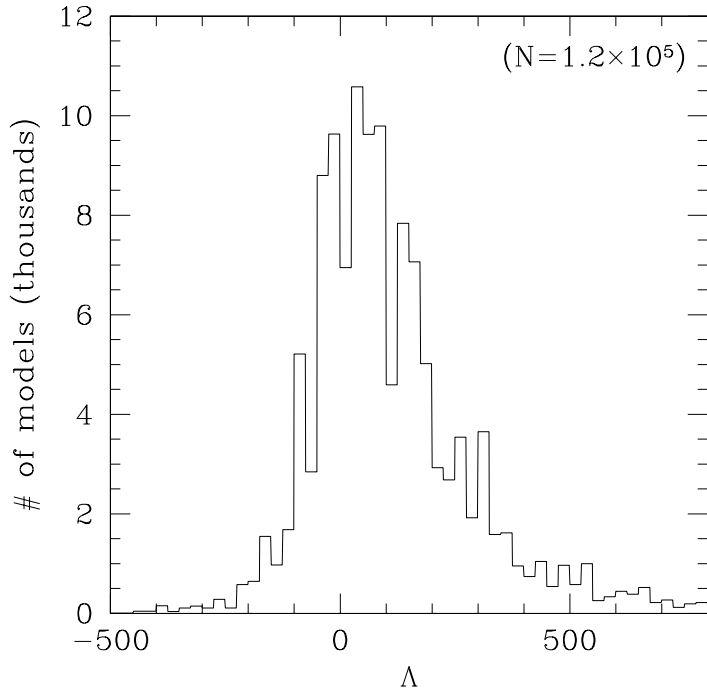


Figure 11: Histogram showing calculated values of the one-loop amplitude Λ defined in Eq. (5.1) across our sample of $N \gtrsim 10^5$ tachyon-free perturbative heterotic string vacua with string-scale supersymmetry breaking. Both positive and negative values of Λ are obtained, with over 73% of models having positive values. The smallest $|\Lambda|$ -value found is $\Lambda \approx 0.0187$, which appears for eight distinct models. (This figure adapted from Ref. [32].)

preference for positive values of Λ , with just over 73% of our models having $\Lambda > 0$. However, we obtained no model with $\Lambda = 0$; indeed, the closest value we obtained for any model is $\Lambda \approx 0.0187$, which appeared for eight distinct models.

Given that we examined more than 10^5 distinct heterotic string models, it is natural to wonder why no smaller values of Λ were found. This question becomes all the more pressing in light of recent expectations [8] that the set of cosmological constant values should be approximately randomly distributed, with relative spacings and a smallest overall value that diminish as additional models are considered.

It is easy to see why this does not happen, however: *just as for gauge groups, it turns out that there is a tremendous degeneracy in the space of string models, with many distinct heterotic string models sharing exactly the same value of Λ .* Again, we stress that these are distinct models with distinct gauge groups and particle content. Nevertheless, such models may give rise to exactly the same one-loop cosmological constant!

The primary means by which two models can have the same cosmological constant

is by having the same set of state degeneracies $\{a_{sd}\}$. This can happen in a number of ways. Recall that these degeneracies represent only the net numbers of bosonic minus fermionic degrees of freedom; thus it is possible for two models to have different numbers of bosons and fermions separately, but to have a common difference between these numbers. Secondly, it is possible for two models to have partition functions $Z_1(\tau)$ and $Z_2(\tau)$ which differ by a purely imaginary function of τ ; in this case, such models they will once again share a common set of state degeneracies $\{a_{sd}\}$ although their values of b_{mn} will differ. Finally, it is possible for $Z_1(\tau)$ and $Z_2(\tau)$ to differ when expressed in terms of conformal field-theory characters (or in terms of Jacobi theta functions ϑ_i), but with this difference proportional to the vanishing Jacobi factor

$$J \equiv \frac{1}{\eta^4} (\vartheta_3^4 - \vartheta_4^4 - \vartheta_2^4) = 0 \quad (5.11)$$

where η and ϑ_i respectively represent the Dedekind eta-function and Jacobi theta-functions, defined as

$$\begin{aligned} \eta(q) &\equiv q^{1/24} \prod_{n=1}^{\infty} (1 - q^n) &= \sum_{n=-\infty}^{\infty} (-1)^n q^{3(n-1/6)^2/2} \\ \vartheta_2(q) &\equiv 2q^{1/8} \prod_{n=1}^{\infty} (1 + q^n)^2 (1 - q^n) &= 2 \sum_{n=0}^{\infty} q^{(n+1/2)^2/2} \\ \vartheta_3(q) &\equiv \prod_{n=1}^{\infty} (1 + q^{n-1/2})^2 (1 - q^n) &= 1 + 2 \sum_{n=1}^{\infty} q^{n^2/2} \\ \vartheta_4(q) &\equiv \prod_{n=1}^{\infty} (1 - q^{n-1/2})^2 (1 - q^n) &= 1 + 2 \sum_{n=1}^{\infty} (-1)^n q^{n^2/2} . \end{aligned} \quad (5.12)$$

Such partition functions $Z_1(\tau)$ and $Z_2(\tau)$ differing by J will then have identical (q, \bar{q}) power-series expansions, once again leading to identical degeneracies $\{a_{sd}\}$ and identical values of Λ .

In Fig. 12, we have plotted the actual numbers of distinct degeneracy sets $\{a_{sd}\}$ found (and therefore the number of distinct cosmological constants Λ obtained) as a function of the number of distinct models examined. It is clear from these results that this cosmological-constant redundancy is quite severe, with only 4303 different values of Λ emerging from over 1.2×10^5 models! This represents a redundancy factor of approximately 28, and it is clear from Fig. 12 that this factor tends to grow larger and larger as the number of examined models increases. Thus, we see that

- **More string models does not necessarily imply more values of Λ .** Indeed, many different string models with entirely different spacetime phenomenologies (different gauge groups, matter representations, hidden sectors, and so forth) exhibit identical values of Λ .

In fact, the shape of the curve in Fig. 12(b) might lead us to conclude that there may be a finite and relatively small number of self-consistent matrices $\{a_{sd}\}$ which

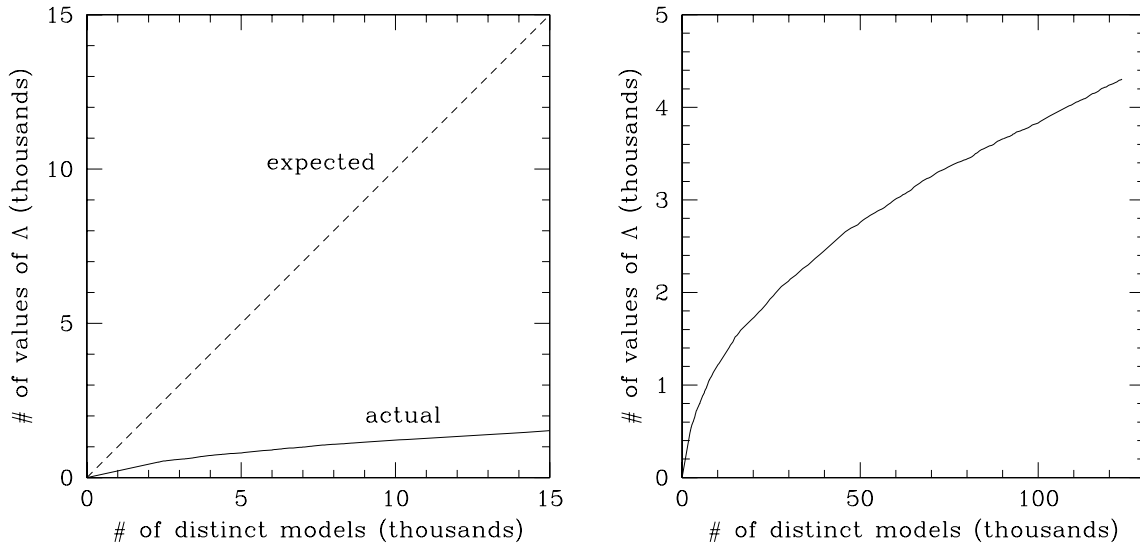


Figure 12: Unexpected degeneracies in the space of non-supersymmetric string vacua. As evident from these figures, there is a tremendous degeneracy according to which many distinct non-supersymmetric heterotic string models with different gauge groups and particle contents nevertheless exhibit exactly the *same* numbers of bosonic and fermionic states and therefore have identical one-loop cosmological constants. (a) (left) Expected versus actual numbers of cosmological constants obtained for the first fifteen thousand models. (b) (right) Continuation of this plot as more models are examined. While the number of models examined is insufficient to calculate a precise shape for this curve, one possibility is that this curve will eventually saturate at a maximum number of allowed cosmological constants, as discussed in the text. (Right figure adapted from Ref. [32].)

our models may be capable of exhibiting. If this were the case, then we would expect the number of such matrices $\{a_{sd}\}$ already seen, Σ , to have a dependence on the total number of models examined, t , of the form

$$\Sigma(t) = N_0 \left(1 - e^{-t/t_0}\right), \quad (5.13)$$

where N_0 is this total number of matrices $\{a_{sd}\}$ and t_0 , the “time constant”, is a parameter characterizing the scale of the redundancy. Fitting the curve in Fig. 12(b) to Eq. (5.13), we find that values of $N_0 \sim 5500$ and $t_0 \sim 70\,000$ seem to be indicated. (One cannot be more precise, since we have clearly not examined a sufficient number of models to observe saturation.) Of course, this sort of analysis assumes that our models uniformly span the space of allowed $\{a_{sd}\}$ matrices (and also that our model set uniformly spans the space of models).

As if this redundancy were not enough, it turns out that there is a further redundancy beyond that illustrated in Fig. 12. In Fig. 12, note that we are actually plotting the numbers of distinct sets of degeneracy matrices $\{a_{sd}\}$, since identical

matrices necessarily imply identical values of Λ . However, it turns out that there are situations in which even *different* values of $\{a_{sd}\}$ can lead to identical values of Λ ! Clearly, such an occurrence would be highly non-trivial, requiring that two sets of integers $\{a_{sd}^{(1)}\}$ and $\{a_{sd}^{(2)}\}$ differ by non-zero integer coefficients $c_{sd} \equiv a_{sd}^{(1)} - a_{sd}^{(2)}$ for which $\sum_{sd} c_{sd} I_{sd} = 0$.

At first glance, given the values of I_{sd} tabulated in Table 2, it may seem that no such integer coefficients c_{sd} could possibly exist. Remarkably, however, it was shown in Ref. [21] that there exists a function

$$Q \equiv \frac{1}{128 \tau_2} \frac{1}{\bar{\eta}^{12} \eta^{24}} \sum_{\substack{i,j,k=2 \\ i \neq j \neq k}}^4 |\vartheta_i|^4 \left\{ \vartheta_i^4 \vartheta_j^4 \vartheta_k^4 \left[2 |\vartheta_j \vartheta_k|^8 - \vartheta_j^8 \overline{\vartheta_k}^8 - \overline{\vartheta_j}^8 \vartheta_k^8 \right] \right. \\ \left. + \vartheta_i^{12} \left[4 \vartheta_i^8 \overline{\vartheta_j}^4 \overline{\vartheta_k}^4 + (-1)^i 13 |\vartheta_j \vartheta_k|^8 \right] \right\} \quad (5.14)$$

which, although non-zero, has the property that

$$\int_{\mathcal{F}} \frac{d^2 \tau}{(\text{Im } \tau)^2} Q = 0 \quad (5.15)$$

as the result of an Atkin-Lehner symmetry [22]. Power-expanding the expression Q in Eq. (5.14) using Eq. (5.12) then yields a set of integer coefficients c_{sd} for which $\sum_{sd} c_{sd} I_{sd} = 0$ as a consequence of Eq. (5.15). Thus, even though neither of the partition functions $Z_1(\tau)$ and $Z_2(\tau)$ of two randomly chosen models exhibits its own Atkin-Lehner symmetry (consistent with an Atkin-Lehner “no-go” theorem [33]), it is possible that their *difference* might nevertheless exhibit such a symmetry. If so, then such models are “twins”, once again sharing the same value of Λ .

As originally reported in Ref. [21], this additional type of twinning redundancy turns out to be pervasive throughout the space of heterotic string models, leading to a further $\sim 15\%$ reduction in the number of distinct values of Λ . Indeed, we find not only twins, but also “triplets” and “quadruplets” — groups of models whose degeneracies $a_{sd}^{(i)}$ differ sequentially through repeated additions of such coefficients c_{sd} . Indeed, we find that our 4303 different sets $\{a_{sd}\}$ which emerge from our $\sim 10^5$ models can be categorized as 3111 “singlets”, 500 groupings of “twins”, 60 groupings of “triplets”, and 3 groupings of “quadruplets”. [Note that indeed $3111 + 2(500) + 3(60) + 4(3) = 4303$.] Thus, the number of distinct cosmological constants emerging from our $\sim 10^5$ models is not actually 4303, but only $3111 + 500 + 60 + 3 = 3674$, which represents an additional 14.6% reduction.

At first glance, since there are relatively few groupings of twins, triplets, and quadruplets, it might seem that this additional reduction is not overly severe. However, this fails to take into account the fact that our previous redundancy may be (and in fact is) statistically clustered around these sets. Indeed, across our entire set of 10^5 distinct string models, we find that

- 30.7% are “singlets”; 48.2% are members of a “twin” grouping; 21.0% are members of a “triplet” grouping; and 0.1% are members of a “quadruplet” grouping.

Thus, we see that this twinning phenomenon is responsible for a massive degeneracy across the space of non-supersymmetric heterotic string vacua.*

Note that this degeneracy may be of considerable relevance for various solutions of the cosmological-constant problem. For example, one proposal in Ref. [10] imagines a large set of degenerate vacua which combine to form a “band” of states whose lowest state has a significantly suppressed vacuum energy. However, the primary ingredient in this formulation is the existence of a large set of degenerate, non-supersymmetric vacua. This is not unlike what we are seeing in this framework. Of course, there still remains the outstanding question concerning how transitions between these vacua can arise, as would be needed in order to generate the required “band” structure.

In all cases, modular invariance is the primary factor that underlies these degeneracies. Despite the vast set of possible heterotic string spectra, there are only so many modular-invariant functions $Z(\tau)$ which can serve as the partition functions for self-consistent string models. It is this modular-invariance constraint which ultimately limits the possibilities for the degeneracy coefficients $\{a_{sd}\}$, and likewise it is modular invariance (along with Atkin-Lehner symmetries) which leads to identities such as Eq. (5.15) which only further enhance this tendency towards degeneracy.

Needless to say, our analysis in this section has been limited to one-loop cosmological constants. It is therefore natural to ask whether such degeneracies might be expected to persist at higher orders. Of course, although modular invariance is a one-loop phenomenon, there exist multi-loop generalizations of modular invariance; likewise it has been speculated that there also exist multi-loop extensions of Atkin-Lehner symmetry [22]. Indeed, modular invariance is nothing but the reflection of the underlying finiteness of the string amplitudes, and we expect this finiteness to persist to any order in the string perturbation expansion. It is therefore possible that degeneracies such as these will persist to higher orders as well.

In any case, this analysis dramatically illustrates that many of our naïve expectations concerning the values of string amplitudes such as the cosmological constant and the distributions of these values may turn out to be grossly inaccurate when confronted with the results of explicit string calculations. The fact that string theory not only provides infinite towers of states but then tightly constrains the properties of these towers through modular symmetries — even when spacetime supersymmetry is broken — clearly transcends our naïve field-theoretic expectations. It is therefore natural to expect that such properties will continue to play a significant role in future statistical studies of the heterotic landscape, even if/when stable non-supersymmetric heterotic string models are eventually constructed.

*Indeed, reviving the “raindrop” analogy introduced in the Introduction, we see that the rain falls mainly on the plane.

6 Gauge groups and cosmological constants: Statistical correlations

We now turn to *correlations* between our gauge groups and cosmological constants. To what extent does the gauge group of a heterotic string model influence the magnitude of its cosmological constant, and vice versa? Note that in field theory, these quantities are completely unrelated — the gauge group is intrinsically non-gravitational, whereas the cosmological constant is of primarily gravitational relevance. However, in string theory, we can expect correlations to occur.

To begin the discussion, let us again construct a “tree” according to which our string models are grouped according to their gauge groups. While in Sect. 4 we grouped our models on “branches” according to their numbers of gauge-group factors, in this section, for pedagogical purposes, we shall instead group our models into “clusters” according to their orders.

- *order=946*: As we know, there is only one distinct string model with this order, with gauge group $SO(44)$. The corresponding cosmological constant is $\Lambda \approx 7800.08 \equiv \Lambda_1$. This is the largest value of Λ for any string model, and it appears for the $SO(44)$ string model only.
- *order=786*: This cluster contains two distinct models, both of which have gauge group $SO(40) \times SU(2)^2$. However, while one of these models has $\Lambda \approx 3340.08$, the other has a cosmological constant exactly equal to $\Lambda_1/2!$
- *order=658*: This cluster contains 12 distinct models, all with gauge group $SO(36) \times SO(8)$. Remarkably, once again, all have cosmological constants $\Lambda = \Lambda_1/2$, even though they differ in their particle representations and content. This is a reflection of the huge cosmological-constant redundancies discussed in Sect. 5.
- *order=642*: This cluster contains only one model, with gauge group $SO(36) \times SU(2)^4$ and cosmological constant $\Lambda \approx 3620.06 \equiv \Lambda_2$.
- *order=578*: Here we have one model with gauge group $SO(34) \times SU(4) \times U(1)^2$. Remarkably, this model has cosmological constant given by $\Lambda = \Lambda_1/4!$

These kinds of redundancies and scaling patterns persist as we continue to implement twists that project out gauge bosons from our string models. For example, we find

- *order=530*: Here we have 10 distinct string models: nine have gauge group $SO(32) \times SO(8) \times SU(2)^2$, while one has gauge group $E_8 \times SO(24) \times SU(2)^2$. Two of the models in the first group have $\Lambda = \Lambda_2$, while the remaining eight models in this cluster exhibit five new values of Λ between them.

- *order=514*: Here we have two distinct string models, both with gauge group $SO(32) \times SU(2)^6$: one has $\Lambda = \Lambda_1/2$, while the other has $\Lambda = \Lambda_1/4$.
- *order=466*: Here we have 12 distinct string models: five with gauge group $SO(24) \times SO(20)$, two with gauge group $E_8 \times SO(20) \times SO(8)$, and five with gauge group $SO(30) \times SU(4)^2 \times U(1)$. All of the models in the last group have $\Lambda = \Lambda_1/4$, while two of the five in the first group have $\Lambda = \Lambda_1/2$. This is also the first cluster in which models with $\Lambda < 0$ appear.

Indeed, as we proceed towards models with smaller orders, we generate not only new values of the cosmological constant, but also cosmological-constant values which are merely rescaled from previous values by factors of 2, 4, 8, and so forth. For example, the original maximum value Λ_1 which appears only for the $SO(44)$ string model has many “descendents”: there are 21 distinct models with $\Lambda = \Lambda_1/2$; 61 distinct models with $\Lambda = \Lambda_1/4$; 106 distinct models with $\Lambda = \Lambda_1/8$; and so forth.

Ultimately, these rescalings are related to the fact that our models are constructed through successive \mathbf{Z}_2 twists. Although there are only limited numbers of modular-invariant partition functions $Z(\tau)$, these functions may be rescaled without breaking the modular invariance. However, we emphasize that *this rescaling of the partition function does not represent a trivial overall rescaling of the associated particle spectrum*. In each model, for example, there can only be one distinct gravity multiplet; likewise, the string vacuum states are necessarily unique. Thus, it is somewhat remarkable that two models with completely different particle spectra can nevertheless give rise to rescaled versions of the same partition function and cosmological constant.

Having described the characteristics of our cosmological-constant tree, let us now turn to its overall statistics and correlations. For each branch of the tree, we can investigate the values of the corresponding cosmological constants, averaged over all models on that branch. If we organize our branches according to the numbers of gauge-group factors as in Sect. 4, we then find the results shown in Figs. 13(a) and 13(b). Alternatively, we can also cluster our models according to the orders of their gauge groups, as described above, and calculate average cosmological constants as a function of these orders. We then find the results shown in Fig. 13(c).

Clearly, we see from Fig. 13 that there is a strong and dramatic correlation between gauge groups and cosmological constants:

- **Models with highly shattered gauge groups and many irreducible gauge-group factors tend to have smaller cosmological constants, while those with larger non-abelian gauge groups tend to have larger cosmological constants.** Indeed, we see from Fig. 13(b) that the average cosmological constant grows approximately linearly with the average rank of the gauge-group factors in the corresponding model.

It is easy to understand this result. As we shatter our gauge groups into smaller irreducible factors, the average size of each *representation* of the gauge group also

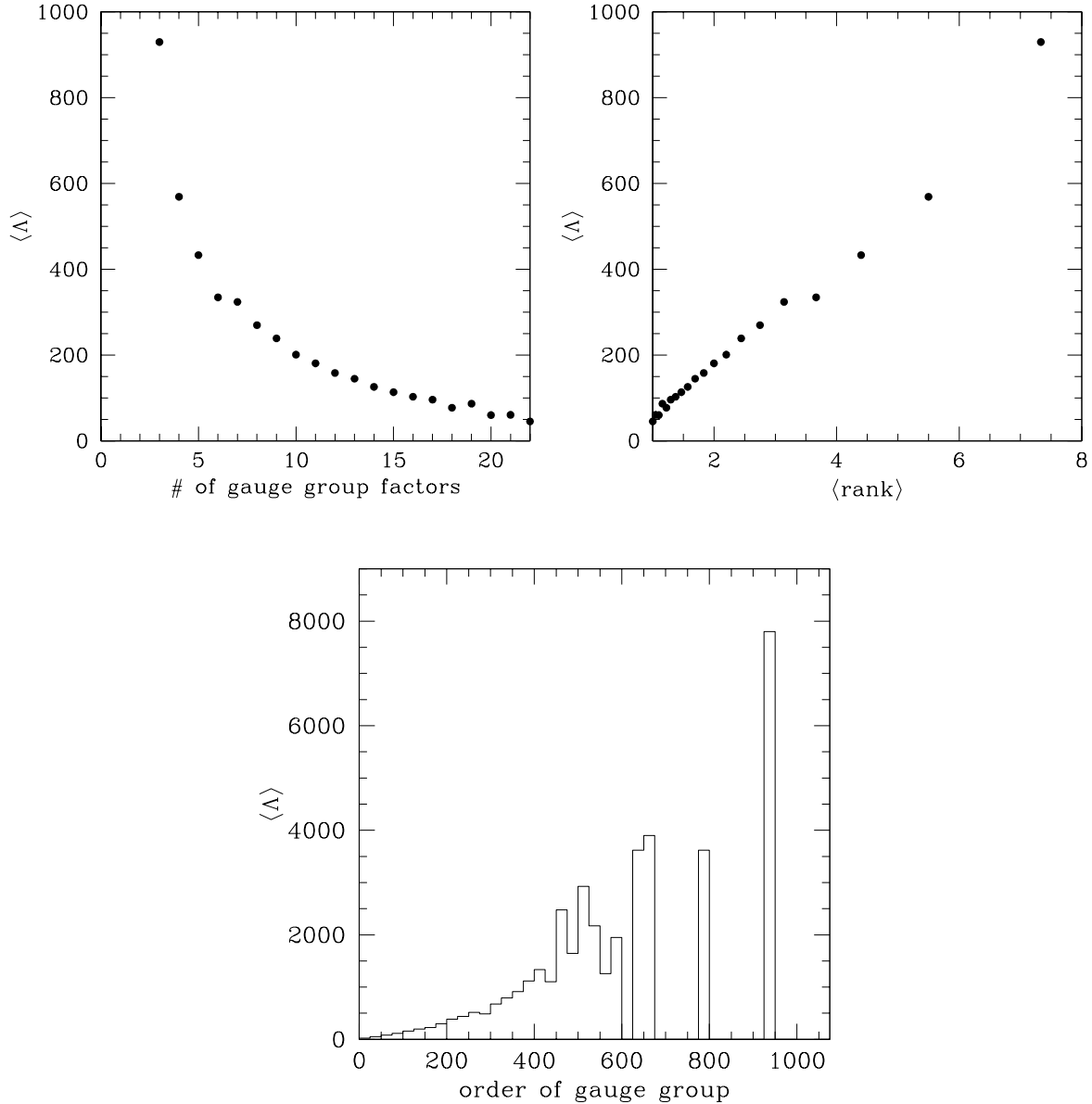


Figure 13: Correlations between cosmological constants and gauge groups. (a) (upper left) Average values of the cosmological constants obtained as a function of the number f of gauge-group factors in the corresponding string models. Note that all cosmological constant averages are positive even though approximately 1/4 of individual string models have $\Lambda < 0$, as shown in Fig. 11. For plotting purposes, we show data only for values $f \geq 3$. (b) (upper right) Same data plotted versus the average rank per gauge group factor, defined as $22/f$. (c) (lower figure) Histogram showing the average values of Λ as a function of the order (dimension) of corresponding gauge group. Note that in every populated bin, we find $\langle \Lambda \rangle > 0$ even though most bins contain at least some string models with $\Lambda < 0$. Thus, in this figure, bins with $\langle \Lambda \rangle = 0$ are to be interpreted as empty rather than as bins for which $\Lambda > 0$ models exactly balance against $\Lambda < 0$ models.

becomes smaller. (For example, we have already seen this behavior in Fig. 8 for gauge bosons in the adjoint representation.) Therefore, we expect the individual tallies of bosonic and fermionic states at each string mass level to become smaller as the total gauge group is increasingly shattered. If these individual numbers of bosons and fermions become smaller, then we statistically expect the magnitudes of their differences $\{a_{sd}\}$ in Eq. (5.7) to become smaller as well. We therefore expect the cosmological constant to be correlated with the degree to which the gauge group of the heterotic string model is shattered, as found in Fig. 13. The fact that the average cosmological grows approximately linearly with the average rank of the gauge-group factors [as shown in Fig. 13(b)] then suggests that on average, this cosmological constant scaling is dominated by vector representations of the gauge groups (whose dimensions grow linearly with the rank of the gauge group). Such representations indeed tend to dominate the string spectrum at the massless level, since larger representations are often excluded on the basis of unitarity grounds for gauge groups with affine levels $k = 1$.

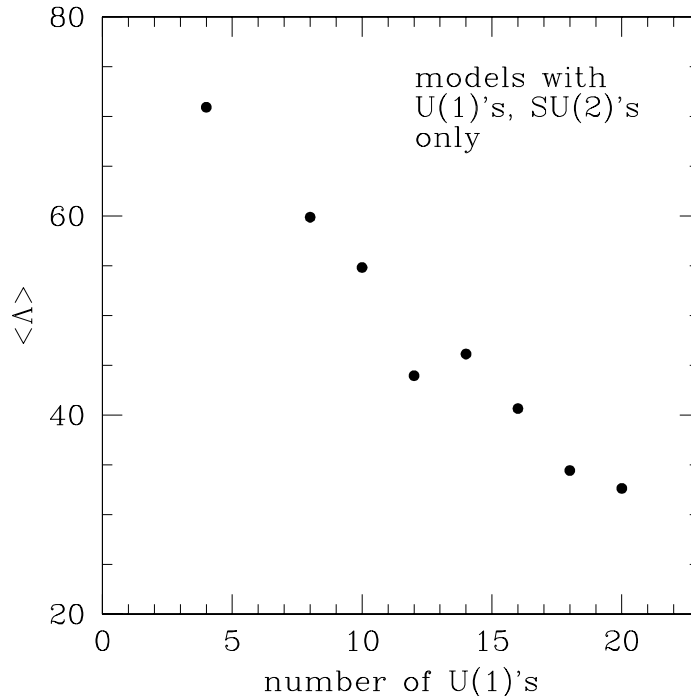


Figure 14: The effects of non-abelianity: Average values of Λ for 12 000 heterotic string models with gauge groups of the form $U(1)^n \times SU(2)^{22-n}$, plotted as a function of n . Since varying n does not change the average rank of each gauge-group factor, this correlation is statistically independent of the correlations shown in Fig. 13.

Even *within* a fixed degree of shattering (*i.e.*, even within a fixed average rank

per gauge group), one may ask whether the degree to which the gauge group is abelian or non-abelian may play a role. In order to pose this question in a way that is independent of the correlations shown in Fig. 13, we can restrict our attention to those heterotic string models in our sample set for which $f = 22$ [*i.e.*, models with gauge groups of the form $U(1)^n \times SU(2)^{22-n}$]. It turns out that there are approximately 12 000 models in this class. Varying n does not change the average rank of each gauge-group factor, and thus any correlation between the cosmological constant and n is statistically independent of the correlations shown in Fig. 13. The results are shown in Fig. 14, averaged over the 12 000 relevant string models. Once again, we see that “bigger” (in this case, non-abelian) groups lead to larger average values of the cosmological constant. The roots of this behavior are the same as those sketched above.

We can also investigate how Λ statistically depends on cross-correlations of gauge groups. Recall that in Table 1, we indicated the percentages of four-dimensional heterotic string models which exhibit various combinations of gauge groups. In Table 3, we indicate the average values of Λ for those corresponding sets of models. We see, once again, that the correlation between average values of Λ and the “size” of our gauge groups is striking. For example, looking along the diagonal in Table 3, we observe that the average values of Λ for models containing gauge groups of the form $G \times G$ always monotonically increase as G changes from $SU(3)$ to $SU(4)$ to $SU(5)$ to $SU(n > 5)$; likewise, the same behavior is observed as G varies from $SO(8)$ to $SO(10)$ to $SO(2n > 10)$. Indeed, as a statistical collection, we see from Table 3 that the models with the largest average values of Λ are those with at least two exceptional factors.

Conversely, scanning across the bottom row of Table 3, we observe that the average value of Λ is minimized for models which contain at least the Standard-Model gauge group $SU(3) \times SU(2) \times U(1)$ among their factors. Given our previous observations about the correlation between the average value of Λ and the size of the corresponding gauge groups, it may seem surprising at first glance that models in which we demand only a single $U(1)$ or $SU(2)$ gauge group do not have an even smaller average value of Λ . However, models for which we require only a single $U(1)$ or $SU(2)$ factor have room for potentially larger gauge-group factors in their complete gauge groups than do models which simultaneously exhibit the factors $U(1) \times SU(2) \times SU(3) \equiv G_{\text{SM}}$. Thus, on average, demanding the appearance of the entire Standard-Model gauge group is more effective in minimizing the resulting average value of Λ than demanding a single $U(1)$ or $SU(2)$ factor alone. In fact, we see from Table 3 that demanding $G_{\text{SM}} \times U(1)$ is even more effective in reducing the average size of Λ , while demanding a completely shattered gauge group of the form $U(1)^n \times SU(2)^{22-n}$ produces averages which are even lower, as shown in Fig. 14.

In this discussion, it is important to stress that we are dealing with statistical *averages*: individual gauge groups and cosmological constants can vary significantly from model to model. In other words, even though we have been plotting average

	U_1	SU_2	SU_3	SU_4	SU_5	$SU_{>5}$	SO_8	SO_{10}	$SO_{>10}$	$E_{6,7,8}$	SM	PS
U_1	104.6	104.6	83.2	112.9	110.7	162.3	131.2	172.1	238.8	342.2	80.8	107.6
SU_2		120.7	80.8	109.1	106.6	157.1	155.5	167.9	282.6	442.5	80.4	103.9
SU_3			85.9	90.9	113.3	136.1	117.6	162.8	193.5	220.2	83.0	88.3
SU_4				115.2	115.0	150.9	129.1	166.7	235.3	314.2	88.9	110.5
SU_5					135.9	156.3	128.1	191.6	199.2	—	107.7	110.3
$SU_{>5}$						200.9	156.4	203.2	274.5	370.7	133.5	142.8
SO_8							192.7	167.5	301.6	442.8	115.3	123.3
SO_{10}								207.8	253.4	289.3	166.0	159.6
$SO_{>10}$									417.4	582.8	190.8	220.0
$E_{6,7,8}$										1165.9	220.2	272.3
SM											82.5	85.5
PS												104.9
total:	108.8	121.4	83.2	113.8	110.7	162.2	163.0	173.0	298.5	440.2	80.8	108.3

Table 3: Average values of Λ for the four-dimensional heterotic string models which exhibit various combinations of gauge groups. This table follows the same organization and notational conventions as Table 1. Interestingly, scanning across the bottom row of this table, we see that those string models which contain at least the Standard-Model gauge group have the smallest average values of Λ .

values of Λ in Figs. 13 and 14, there may be significant standard deviations in these plots. In order to understand the origin of these standard deviations, let us consider the “inverse” of Fig. 13(a) which can be constructed by binning our heterotic string models according to their values of Λ and then plotting the average value of f , the number of gauge-group factors, for the models in each bin. The result is shown in Fig. 15, where we have plotted not only the average values of f but also the corresponding standard deviations. Once again, we see that smaller values of $|\Lambda|$ are clearly correlated with increasingly shattered gauge groups. However, while a particular value of Λ is directly correlated with a contiguous, relatively small range for f , the reverse is not true: a particular value of f is correlated with *two* distinct ranges for Λ of opposite signs. Indeed, even the central magnitudes for Λ in these two ranges are unequal because of the asymmetry of the data in Fig. 15, with the “ascending” portion of the curve having a steeper slope than the descending portion. As a result of this asymmetry, and as a result of the different numbers of string models which populate these two regions, the total value $\langle \Lambda \rangle$ averaged across these two regions does not cancel, but instead follows the curve in Fig. 13(a). Thus, while the curves in Figs. 13 and 14 technically have large standard deviations, we have not shown these standard deviations because they do not reflect large uncertainties in the corresponding allowed values of Λ . Rather, they merely reflect the fact that the allowed values of Λ come from two disjoint but relatively well-focused regions.

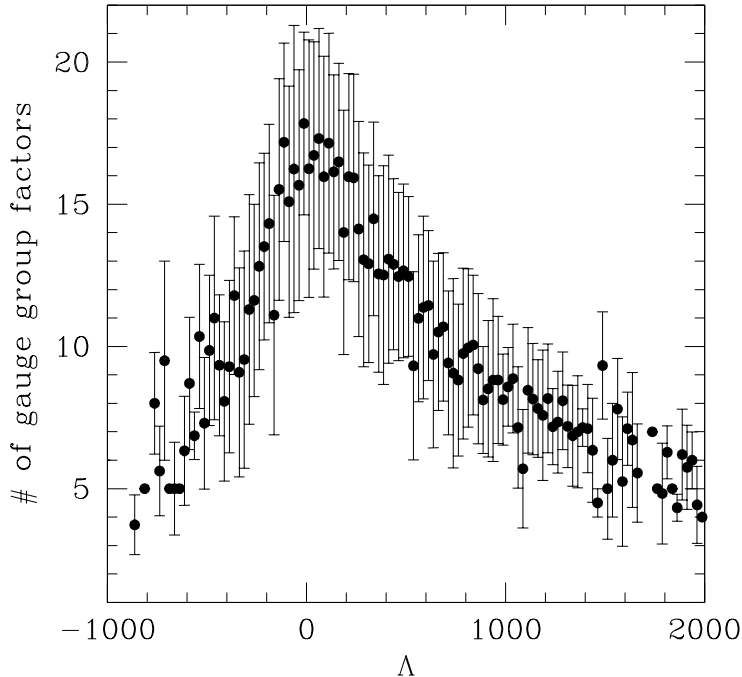


Figure 15: The “inverse” of Fig. 13(a): Here we have binned our heterotic string models according to their values of Λ and then plotted $\langle f \rangle$, the average value of the number of gauge-group factors, for the models in each bin. The error bars delimit the range $\langle f \rangle \pm \sigma$ where σ are the corresponding standard deviations. We see that while a particular value of Λ restricts f to a fairly narrow range, a particular value of f only focuses Λ to lie within two separate ranges of different central magnitudes $|\Lambda|$ and opposite signs.

Of course, as we approach the “top” of the curve in Fig. 15 near $|\Lambda| \approx 0$, these two distinct regions merge together. However, even in this limit, it turns out that the sizes of the standard deviations depend on which physical quantity in the comparison is treated as the independent variable and held fixed. For example, if we restrict our attention to heterotic string models containing a gauge group of the form $U(1)^n \times SU(2)^{22-n}$ (essentially holding f , the number of gauge-group factors, fixed at $f = 22$), we still find corresponding values of Λ populating the rather wide range $-400 \lesssim \Lambda \lesssim 500$. In other words, holding f fixed does relatively little to focus Λ . By contrast, we have already remarked in Sect. 5 that across our entire sample of $\sim 10^5$ models, the smallest value of $|\Lambda|$ that we find is $\Lambda \approx 0.0187$. This value emerges for nine models, eight of which share the same state degeneracies $\{a_{sd}\}$ and one of which is their “twin” (as defined at the end of Sect. 5). If we take Λ as the independent variable and hold $\Lambda \approx 0.0187$ fixed (which represents only one very narrow slice within the bins shown in Fig. 15), we then find that essentially *all* of the correspond-

ing gauge groups are extremely “small”: four are of the form $U(1)^n \times SU(2)^{22-n}$ with $n = 12, 13, 15, 17$, and the only two others are $SU(3) \times SU(2)^4 \times U(1)^{16}$ and $SU(3)^2 \times SU(2)^3 \times U(1)^{15}$. In other words, models with $\Lambda \approx 0.0187$ have $\langle f \rangle \approx 21.67$, with only a very small standard deviation. Indeed, amongst all distinct models with $|\Lambda| \leq 0.04$, we find none with gauge-group factors of rank exceeding 5; only 8.2% of such models have an individual gauge-group factor of rank exceeding 3 and only 1.6% have an individual gauge-group factor of rank exceeding 4. None were found that exhibited any larger gauge-group factors. Thus, we see that keeping Λ small goes a long way towards keeping the corresponding gauge-group factors small.

It is, of course, dangerous to extrapolate from these observations of $\sim 10^5$ models in order to make claims concerning a full string landscape which may consist of $\sim 10^{500}$ models or more. Nevertheless, as we discussed at the end of Sect 2, we have verified that all of these statistical correlations appear to have reached the “continuum limit” (meaning that they appear to be numerically stable as more and more string models are added to our sample set). Indeed, although the precise minimum value of $|\Lambda|$ is likely to continue to decline as more and more models are examined, the correlation between small values of $|\Lambda|$ and small gauge groups is likely to persist. Needless to say, it is impossible to estimate how large our set of heterotic string models must become before we randomly find a model with $|\Lambda| \approx 10^{-120}$; indeed, if the curve in Fig. 12 truly saturates at a finite value, such models may not even exist. However, if we assume (as in Ref. [8]) that such models exist — providing what would truly be a stable string “vacuum” — then it seems overwhelmingly likely that

- **Perturbative heterotic string vacua with observationally acceptable cosmological constants can be expected to have extremely small gauge-group factors, with $U(1)$, $SU(2)$, and $SU(3)$ overwhelmingly favored relative to larger groups such as $SU(5)$, $SO(10)$, or $E_{6,7,8}$. Thus, for such string vacua, the Standard-Model gauge group is much more likely to be realized at the string scale than any of its grand-unified extensions.**

As always, such a claim is subject to a number of additional assumptions: we are limited to perturbative heterotic string vacua, we are examining only one-loop string amplitudes, and so forth. Nevertheless, we find this type of correlation to be extremely intriguing, and feel that it is likely to hold for higher-loop contributions to the vacuum amplitude as well.

Note, in particular, that the critical ingredient in this claim is the assumption of small cosmological constant. Otherwise, statistically weighting all of our string models equally without regard for their cosmological constants, we already found in Sect. 4 that the Standard Model is relatively *disfavored*, appearing only 10% of the time, while the $SO(2n \geq 10)$ GUT groups appear with the much greater frequency 24.5%. Thus, it is the requirement of a small cosmological constant which is responsible for redistributing these probabilities in such a dramatic fashion.

There is, however, another possible way to interpret this correlation between the magnitudes of Λ and the sizes of gauge groups. As we have seen, smaller values of Λ tend to emerge as the gauge group becomes increasingly shattered. However, as we know, there is a fundamental limit to how shattered our gauge groups can become: f simply cannot exceed 22, *i.e.*, there is no possible gauge-group factor with rank less than 1. Thus, the correlation between Λ and average gauge-group rank may imply that there is likewise a minimum possible value for Λ . If so, it is extremely unlikely that perturbative heterotic string models will be found in which Λ is orders of magnitude less than the values we have already seen.

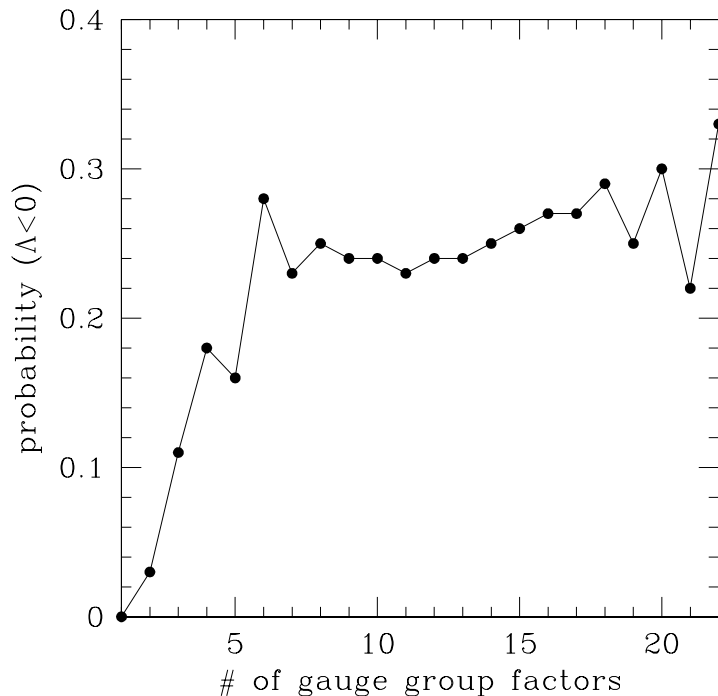


Figure 16: The probability that a randomly chosen heterotic string model has a negative value of Λ (*i.e.*, a positive value of the vacuum energy density λ), plotted as a function of the number of gauge-group factors in the total gauge group of the model. We see that we do not have a significant probability of obtaining models with $\Lambda < 0$ until our gauge group is “shattered” into at least four or five factors; this probability then remains roughly independent of the number of factors as further shattering occurs.

Another important characteristic of such string models is the *sign* of Λ . For example, whether the vacuum energy $\lambda = -\frac{1}{2}\mathcal{M}^4\Lambda$ is positive or negative can determine whether the corresponding spacetime is de Sitter (dS) or anti-de Sitter (AdS). In Fig. 16, we show the probability that a randomly chosen heterotic string model has a negative value of Λ , plotted as a function of the number of gauge-group factors in

the total gauge group of the model. For small numbers of factors, the corresponding models all tend to have very large positive values of Λ . Indeed, as indicated in Fig. 16, we do not accrue a significant probability of obtaining models with $\Lambda < 0$ until our gauge group is “shattered” into at least four or five factors. The probability of obtaining negative values of Λ then saturates near $\approx 1/4$, remaining roughly independent of the number of gauge-group factors as further shattering occurs. Thus, we see that regardless of the value of f , the “ascending” portion of Fig. 15 is populated by only a quarter as many models as populate the “descending” portion. Since the overwhelming majority of models have relatively large numbers of gauge-group factors (as indicated in Fig. 1), we see that on average, approximately 1/4 of our models have negative values of Λ . This is consistent with the histogram in Fig. 11.

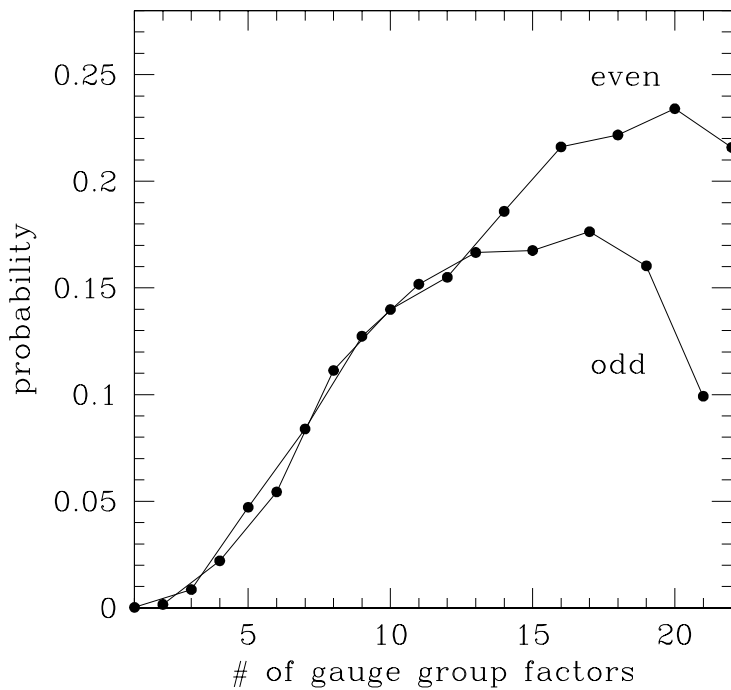


Figure 17: The degeneracy of values of the cosmological constant relative to gauge groups. We plot the probability that a given value of Λ (chosen from amongst the total set of obtained values) will emerge from a model with f gauge-group factors, as a function of f for even and odd values of f . This probability is equivalently defined as the number of distinct Λ values obtained from models with f gauge-group factors, divided by the total number of Λ values found across all values of f . The resemblance of these curves to those in Fig. 1 indicates that the vast degeneracy of cosmological-constant values is spread approximately uniformly across models with different numbers of gauge-group factors.

Finally, we can investigate how the vast redundancy in the values of the cosmo-

logical constant is correlated with the corresponding gauge groups and the degree to which they are shattered. In Fig. 17, we plot the number of distinct Λ values obtained from models with f gauge-group factors, divided by the total number of Λ values found across all values of f . Note that the sum of the probabilities plotted in Fig. 17 exceeds one. This is because a given value of Λ may emerge from models with many different values of f — *i.e.*, the sets of values of Λ for each value of f are not exclusive. It turns out that this is a huge effect, especially as f becomes relatively large.

The fact that the curves in Fig. 1 and Fig. 17 have similar shapes as functions of f implies that the vast degeneracy of cosmological-constant values is spread approximately uniformly across models with different numbers of gauge-group factors. Moreover, as indicated in Fig. 12(b), this degeneracy factor itself tends to decrease as more and more models are examined, leading to a possible saturation of distinct Λ values, as discussed above.

7 Discussion

In this paper, we have investigated the statistical properties of a fairly large class of perturbative, four-dimensional, non-supersymmetric, tachyon-free heterotic string models. We focused on their gauge groups, their one-loop cosmological constants, and the statistical correlations that emerge between these otherwise disconnected quantities.

Clearly, as stated in the Introduction, much more work remains to be done, even within this class of models. For example, it would be of immediate interest to examine other aspects of the full particle spectra of these models and obtain statistical information concerning Standard-Model embeddings, spacetime chirality, numbers of generations, and $U(1)$ hypercharge assignments, as well as cross-correlations between these quantities. This would be analogous to what has been done for Type I orientifold models in Refs. [5, 6]. One could also imagine looking at the gauge couplings and their runnings, along with their threshold corrections [30], to see whether it is likely that unification occurs given low-energy precision data [29, 34]. It would also be interesting to examine the properties of the cosmological constant *beyond* one-loop order, with an eye towards understanding to what extent the unexpected degeneracies we have found persist. An analysis of other string amplitudes and correlation functions is clearly also of interest, particularly as they relate to Yukawa couplings and other phenomenological features. Indeed, a more sophisticated analysis examining all of these features with a significantly larger sample set of models is currently underway [35].

Needless to say, another option is to expand the class of heterotic string models under investigation. While the models examined in this paper are all non-supersymmetric, it is also important to repeat much of this work for four-dimensional heterotic models with $\mathcal{N} = 1$, $\mathcal{N} = 2$, and $\mathcal{N} = 4$ supersymmetry. There are two

distinct reasons why this is an important undertaking. First, because they are supersymmetric, such models are commonly believed to be more relevant to particle physics in addressing issues of gauge coupling unification and the gauge hierarchy problem. But secondly, at a more mathematical level, such models have increased stability properties relative to the non-supersymmetric models we have been examining here. Thus, by examining the statistical properties of such models and comparing them with the statistical properties of supersymmetric models, we can determine the extent to which supersymmetry has an effect on these other phenomenological features. Such analyses are also underway [35]. Indeed, in many cases these perturbative supersymmetric heterotic strings are dual to other strings (*e.g.*, Type I orientifold models) whose statistical properties are also being analyzed. Thus, analysis of the perturbative heterotic landscape, both supersymmetric and non-supersymmetric, will enable *statistical* tests of duality symmetries across the entire string landscape.

Beyond this, of course, there are many broader classes of closed string models which may be examined — some of these are discussed in Sect. 2. Indeed, of great interest are completely *stable* non-supersymmetric models. As discussed in Ref. [36], such models could potentially provide *non-supersymmetric* solutions not only for the cosmological-constant problem, but also for the apparent gauge hierarchy problem. Such models could therefore provide a framework for an alternative, non-supersymmetric approach towards string phenomenology [36]. However, given that no entirely stable non-supersymmetric perturbative heterotic string models have yet been constructed, the analysis of this paper represents the current “state of the art” as far as non-supersymmetric perturbative heterotic string model-building is concerned.

As mentioned in the Introduction, this work may be viewed as part of a larger “string vacuum project” whose goal is to map out the properties of the landscape of string vacua. It therefore seems appropriate to close with two warnings concerning the uses and abuses of such large-scale statistical studies as a method of learning about the properties of the landscape.

The first warning concerns what may be called “lamppost” effect — the danger of restricting one’s attention to only those portions of the landscape where one has control over calculational techniques. (This has been compared to searching for a small object in the darkness of night: the missing object may be elsewhere, but the region under the lamppost may represent the only location where the search can be conducted at all.) For example, our analysis in this paper has been restricted to string models exploiting “free-field” constructions (such as string constructions using bosonic lattices or free-fermionic formalisms). While this class of string models is very broad and lends itself naturally to a computer-automated search and analysis, it is entirely possible that the models with the most interesting phenomenologies are beyond such a class. Indeed, it is very easy to imagine that different constructions will have different strengths and weaknesses as far as their low-energy phenomenologies are concerned, and that one type of construction may easily realize features that

another cannot accommodate.

By contrast, the second danger can be called the “Gödel effect” — the danger that no matter how many conditions (or input “priors”) one demands for a phenomenologically realistic string model, there will always be another observable for which the set of realistic models will make differing predictions. Therefore, such an observable will remain beyond our statistical ability to predict. (This is reminiscent of the “Gödel incompleteness theorem” which states that in any axiomatic system, there is always another statement which, although true, cannot be deduced purely from the axioms.) Given that the full string landscape is very large, consisting of perhaps 10^{500} distinct models or more, the Gödel effect may represent a very real danger. Thus, since one can never be truly sure of having examined a sufficiently sizable portion of the landscape, it is likewise never absolutely clear whether we can be truly free of such Gödel-type ambiguities when attempting to make string predictions.

Of course, implicit in each of these effects is the belief that one actually knows what one is looking for — that we know *which* theory of particle physics should be embedded directly into the string framework and viewed as emerging from a particular string vacuum. However, it is possible that nature might pass through many layers of effective field theories at higher and higher energy scales before reaching an ultimate string-theory embedding. In such cases, the potential constraints on a viable string vacuum are undoubtedly weaker.

Nevertheless, we believe that there are many valid purposes for such statistical studies of actual string models. First, as we have seen at various points in this paper, it is only by examining actual string models — and not effective supergravity solutions — that many surprising features come to light. Indeed, one overwhelming lesson that might be taken from the analysis in this paper is that the string landscape is a very rich place, full of unanticipated properties and characteristics that emerge only from direct analysis of concrete string models.

Second, through their direct enumeration, we gain valuable experience in the construction and analysis of phenomenologically viable models. This is, in some sense, a direct test of string theory as a phenomenological theory of physics. For example, it is clear from the results of this paper that obtaining the Standard-Model gauge group is a fairly non-trivial task within free-field constructions based on \mathbf{Z}_2 periodic/antiperiodic orbifold twists; as we have seen in Fig. 6(b), one must induce a significant amount of gauge-group shattering before a sizable population of models with the Standard-Model gauge group emerges. This could not have been anticipated on the basis of low-energy effective field theories alone, and is ultimately a reflection of worldsheet model-building constraints. Such knowledge and experience are extremely valuable for string model-builders, and can serve as useful guideposts.

Third, as string phenomenologists, we must ultimately come to terms with the landscape. Given that such large numbers of string vacua exist, it is imperative that string theorists learn about these vacua and the space of resulting possibilities. Indeed, the first step in any scientific examination of a large data set is that of

enumeration and classification; this has been true in branches of science ranging from astrophysics and botany to zoology. It is no different here.

But finally, we are justified in interpreting observed statistical correlations as general landscape features to the extent that we can attribute such correlations to the existence of underlying string-theoretic consistency constraints. Indeed, when the constraint operates only within a single class of strings, then the corresponding statistical correlation is likely to hold across only that restricted portion of the landscape. For example, in cases where we were able to interpret our statistical correlations about gauge groups and cosmological constants as resulting from deeper constraints such as conformal and modular invariance, we expect these correlations to hold across the entire space of perturbative closed-string vacua. As such, we may then claim to have extracted true phenomenological predictions from string theory. This is especially true when the string-correlated quantities would have been completely disconnected in quantum field theory.

Thus, it is our belief that such statistical landscape studies have their place, particularly when the results of such studies are interpreted correctly and in the proper context. As such, we hope that this initial study of the perturbative heterotic landscape may represent one small step in this direction.

Acknowledgments

Portions of this work were originally presented at the String Phenomenology Workshop at the Perimeter Institute in April 2005, at the Munich String Phenomenology Conference in August 2005, and at the Ohio State String Landscape Conference in October 2005. This work is supported in part by the National Science Foundation under Grant PHY/0301998, by the Department of Energy under Grant DE-FG02-04ER-41298, and by a Research Innovation Award from Research Corporation. I am happy to thank R. Blumenhagen, M. Douglas, S. Giddings, J. Kumar, G. Shiu, S. Thomas, H. Tye, and especially M. Lennek for discussions. I am also particularly grateful to D. Sénéchal for use of the computer programs [20] which were employed fifteen years ago [21] to generate these string models and to determine their gauge groups. While some of this data was briefly mentioned in Ref. [21], the bulk of the data remained untouched. Because of its prohibitively huge size (over 4 megabytes in 1990!), this data was safely offloaded for posterity onto a standard nine-track magnetic computer tape. I am therefore also extremely grateful to M. Eklund and P. Goisman for their heroic efforts in 2005 to locate the only remaining tape drive within hundreds of miles capable of reading such a fifteen-year-old computer artifact, and to S. Sorenson for having maintained such a tape reader in his electronic antiquities collection and using it to resurrect the data on which this statistical analysis was based.

References

- [1] L. Susskind, arXiv:hep-th/0302219.
For popular introductions, see:
R. Bousso and J. Polchinski, *Sci. Am.* **291**, 60 (2004);
S. Weinberg, arXiv:hep-th/0511037.
- [2] M. R. Douglas, *JHEP* **0305**, 046 (2003) [arXiv:hep-th/0303194];
S. Ashok and M. R. Douglas, *JHEP* **0401**, 060 (2004) [arXiv:hep-th/0307049];
F. Denef and M. R. Douglas, *JHEP* **0405**, 072 (2004) [arXiv:hep-th/0404116];
A. Giriyavets, S. Kachru and P. K. Tripathy, *JHEP* **0408**, 002 (2004) [arXiv:hep-th/0404243];
D. Robbins and S. Sethi, *Phys. Rev. D* **71**, 046008 (2005) [arXiv:hep-th/0405011];
A. Misra and A. Nanda, *Fortsch. Phys.* **53**, 246 (2005) [arXiv:hep-th/0407252];
M. R. Douglas, *Comptes Rendus Physique* **5**, 965 (2004) [arXiv:hep-th/0409207];
J. P. Conlon and F. Quevedo, *JHEP* **0410**, 039 (2004) [arXiv:hep-th/0409215];
J. Kumar and J. D. Wells, *Phys. Rev. D* **71**, 026009 (2005) [arXiv:hep-th/0409218]; *JHEP* **0509**, 067 (2005) [arXiv:hep-th/0506252];
G. Dvali, arXiv:hep-th/0410286;
O. DeWolfe, A. Giriyavets, S. Kachru and W. Taylor, *JHEP* **0502**, 037 (2005) [arXiv:hep-th/0411061];
F. Denef and M. R. Douglas, *JHEP* **0503**, 061 (2005) [arXiv:hep-th/0411183];
B. S. Acharya, F. Denef and R. Valandro, *JHEP* **0506**, 056 (2005) [arXiv:hep-th/0502060];
F. Denef and M. R. Douglas, arXiv:hep-th/0602072.
- [3] M. R. Douglas, arXiv:hep-th/0405279;
M. Dine, E. Gorbatov and S. D. Thomas, arXiv:hep-th/0407043;
M. Dine, D. O’Neil and Z. Sun, *JHEP* **0507**, 014 (2005) [arXiv:hep-th/0501214];
JHEP **0601**, 162 (2006) [arXiv:hep-th/0505202];
M. Dine and Z. Sun, *JHEP* **0601**, 129 (2006) [arXiv:hep-th/0506246].
- [4] N. Arkani-Hamed and S. Dimopoulos, *JHEP* **0506**, 073 (2005) [arXiv:hep-th/0405159];
G. F. Giudice and A. Romanino, *Nucl. Phys. B* **699**, 65 (2004) [Erratum-ibid. *B* **706**, 65 (2005)] [arXiv:hep-ph/0406088];
J. D. Wells, *Phys. Rev. D* **71**, 015013 (2005) [arXiv:hep-ph/0411041].
- [5] R. Blumenhagen, F. Gmeiner, G. Honecker, D. Lust and T. Weigand, *Nucl. Phys. B* **713**, 83 (2005) [arXiv:hep-th/0411173];
F. Gmeiner, R. Blumenhagen, G. Honecker, D. Lust and T. Weigand, *JHEP* **0601**, 004 (2006) [arXiv:hep-th/0510170].

- [6] T. P. T. Dijkstra, L. R. Huiszoon and A. N. Schellekens, Phys. Lett. B **609**, 408 (2005) [arXiv:hep-th/0403196]; Nucl. Phys. B **710**, 3 (2005) [arXiv:hep-th/0411129].
- [7] S. Weinberg, Phys. Rev. Lett. **59**, 2607 (1987);
 A. Vilenkin, Phys. Rev. Lett. **74**, 846 (1995) [arXiv:gr-qc/9406010];
 V. Agrawal, S. M. Barr, J. F. Donoghue and D. Seckel, Phys. Rev. Lett. **80**, 1822 (1998) [arXiv:hep-ph/9801253];
 S. Weinberg, Phys. Rev. D **61**, 103505 (2000) [arXiv:astro-ph/0002387];
 M. L. Graesser, S. D. H. Hsu, A. Jenkins and M. B. Wise, Phys. Lett. B **600**, 15 (2004) [arXiv:hep-th/0407174].
 For a review, see: S. Weinberg, Rev. Mod. Phys. **61**, 1 (1989).
- [8] R. Bousso and J. Polchinski, JHEP **0006**, 006 (2000) [arXiv:hep-th/0004134];
 J. L. Feng, J. March-Russell, S. Sethi and F. Wilczek, Nucl. Phys. B **602**, 307 (2001) [arXiv:hep-th/0005276].
- [9] J. F. Donoghue, JHEP **0008**, 022 (2000) [arXiv:hep-ph/0006088];
 T. Banks, M. Dine and L. Motl, JHEP **0101**, 031 (2001) [arXiv:hep-th/0007206];
 J. Garriga and A. Vilenkin, Phys. Rev. D **64**, 023517 (2001) [arXiv:hep-th/0011262];
 S. Dimopoulos and S. D. Thomas, Phys. Lett. B **573**, 13 (2003) [arXiv:hep-th/0307004];
 H. Firouzjahi, S. Sarangi and S. H. H. Tye, JHEP **0409**, 060 (2004) [arXiv:hep-th/0406107];
 V. Balasubramanian and P. Berglund, JHEP **0411**, 085 (2004) [arXiv:hep-th/0408054];
 A. Kobakhidze and L. Mersini-Houghton, arXiv:hep-th/0410213;
 L. Mersini-Houghton, Class. Quant. Grav. **22**, 3481 (2005) [arXiv:hep-th/0504026];
 J. Garriga and A. Vilenkin, arXiv:hep-th/0508005;
 P. Castelo Ferreira and P. Vargas Moniz, arXiv:hep-th/0601070;
 arXiv:hep-th/0601086;
 D. Schwartz-Perlov and A. Vilenkin, arXiv:hep-th/0601162.
- [10] G. L. Kane, M. J. Perry and A. N. Zytchow, arXiv:hep-th/0311152.
- [11] K. R. Dienes, E. Dudas and T. Gherghetta, Phys. Rev. D **72**, 026005 (2005) [arXiv:hep-th/0412185];
 N. Arkani-Hamed, S. Dimopoulos and S. Kachru, arXiv:hep-th/0501082;
 J. Distler and U. Varadarajan, arXiv:hep-th/0507090.
- [12] T. Banks, M. Dine and E. Gorbatov, JHEP **0408**, 058 (2004) [arXiv:hep-th/0309170];

- B. Freivogel and L. Susskind, Phys. Rev. D **70**, 126007 (2004) [arXiv:hep-th/0408133];
 B. Freivogel, M. Kleban, M. Rodriguez Martinez and L. Susskind, arXiv:hep-th/0505232;
 B. Feldstein, L. J. Hall and T. Watari, Phys. Rev. D **72**, 123506 (2005) [arXiv:hep-th/0506235].
- [13] T. Banks, arXiv:hep-th/0412129;
 C. Vafa, arXiv:hep-th/0509212.
- [14] For a recent review, see:
 J. Kumar, arXiv:hep-th/0601053.
- [15] The European String Vacuum Project website is located at <http://www.ippp.dur.ac.uk/~dgrell/svp/>. (The North American SVP website is still under development.)
- [16] S. B. Giddings, S. Kachru and J. Polchinski, Phys. Rev. D **66**, 106006 (2002) [arXiv:hep-th/0105097];
 K. Becker and M. Becker, JHEP **0107**, 038 (2001) [arXiv:hep-th/0107044];
 K. Becker, M. Becker, M. Haack and J. Louis, JHEP **0206**, 060 (2002) [arXiv:hep-th/0204254];
 S. Kachru, M. B. Schulz and S. Trivedi, JHEP **0310**, 007 (2003) [arXiv:hep-th/0201028];
 S. Kachru, R. Kallosh, A. Linde and S. P. Trivedi, Phys. Rev. D **68**, 046005 (2003) [arXiv:hep-th/0301240];
 R. Blumenhagen, D. Lust and T. R. Taylor, Nucl. Phys. B **663**, 319 (2003) [arXiv:hep-th/0303016];
 J. F. G. Cascales and A. M. Uranga, JHEP **0305**, 011 (2003) [arXiv:hep-th/0303024];
 P. G. Camara, L. E. Ibanez and A. M. Uranga, Nucl. Phys. B **689**, 195 (2004) [arXiv:hep-th/0311241]; Nucl. Phys. B **708**, 268 (2005) [arXiv:hep-th/0408036];
 M. Grana, T. W. Grimm, H. Jockers and J. Louis, Nucl. Phys. B **690**, 21 (2004) [arXiv:hep-th/0312232];
 F. Marchesano and G. Shiu, Phys. Rev. D **71**, 011701 (2005) [arXiv:hep-th/0408059]; JHEP **0411**, 041 (2004) [arXiv:hep-th/0409132];
 A. Font, JHEP **0411**, 077 (2004) [arXiv:hep-th/0410206];
 F. Marchesano, G. Shiu and L. T. Wang, Nucl. Phys. B **712**, 20 (2005) [arXiv:hep-th/0411080];
 M. Cvetič, T. Li and T. Liu, Phys. Rev. D **71**, 106008 (2005) [arXiv:hep-th/0501041];
 V. Balasubramanian, P. Berglund, J. P. Conlon and F. Quevedo, JHEP **0503**, 007 (2005) [arXiv:hep-th/0502058];

- K. Choi, A. Falkowski, H. P. Nilles and M. Olechowski, Nucl. Phys. B **718**, 113 (2005) [arXiv:hep-th/0503216];
 J. P. Conlon, F. Quevedo and K. Suruliz, JHEP **0508**, 007 (2005) [arXiv:hep-th/0505076];
 A. Falkowski, O. Lebedev and Y. Mambrini, JHEP **0511**, 034 (2005) [arXiv:hep-ph/0507110];
 C. P. Burgess, C. Escoda and F. Quevedo, arXiv:hep-th/0510213;
 J. J. Blanco-Pillado, R. Kallosh and A. Linde, arXiv:hep-th/0511042;
 B. C. Allanach, F. Quevedo and K. Suruliz, arXiv:hep-ph/0512081.
- [17] For recent reviews, see:
 R. Blumenhagen, M. Cvetič, P. Langacker and G. Shiu, arXiv:hep-th/0502005;
 M. Grana, Phys. Rept. **423**, 91 (2006) [arXiv:hep-th/0509003].
- [18] L. Alvarez-Gaume, P. H. Ginsparg, G. W. Moore and C. Vafa, Phys. Lett. B **171**, 155 (1986);
 L. J. Dixon and J. A. Harvey, Nucl. Phys. B **274**, 93 (1986).
- [19] H. Kawai, D. C. Lewellen and S. H. H. Tye, Nucl. Phys. B **288**, 1 (1987);
 I. Antoniadis, C. P. Bachas and C. Kounnas, Nucl. Phys. B **289**, 87 (1987);
 H. Kawai, D. C. Lewellen, J. A. Schwartz and S. H. H. Tye, Nucl. Phys. B **299**, 431 (1988).
- [20] D. S en echal, Phys. Rev. D **39**, 3717 (1989).
- [21] K. R. Dienes, Phys. Rev. Lett. **65**, 1979 (1990).
- [22] G. W. Moore, Nucl. Phys. B **293**, 139 (1987) [Erratum-ibid. B **299**, 847 (1988)];
 K. R. Dienes, Phys. Rev. D **42**, 2004 (1990).
- [23] K. S. Narain, Phys. Lett. B **169**, 41 (1986);
 K. S. Narain, M. H. Sarmadi and E. Witten, Nucl. Phys. B **279**, 369 (1987).
- [24] W. Lerche, D. Lust and A. N. Schellekens, Nucl. Phys. B **287**, 477 (1987).
- [25] H. Kawai, D. C. Lewellen and S. H. H. Tye, Phys. Rev. D **34**, 3794 (1986).
- [26] Z. S. Li and C. S. Lam, Int. J. Mod. Phys. A **7**, 5739 (1992) [Erratum-ibid. A **7**, 8081 (1992)];
 Z. Kakushadze, G. Shiu and S. H. H. Tye, Phys. Rev. D **54**, 7545 (1996) [arXiv:hep-th/9607137].
- [27] A. E. Faraggi, Phys. Lett. B **278**, 131 (1992); Phys. Lett. B **274**, 47 (1992).

- [28] D. C. Lewellen, Nucl. Phys. B **337**, 61 (1990);
 K. R. Dienes and J. March-Russell, Nucl. Phys. B **479**, 113 (1996) [arXiv:hep-th/9604112];
 K. R. Dienes, Nucl. Phys. B **488**, 141 (1997) [arXiv:hep-ph/9606467].
- [29] For a review, see:
 K. R. Dienes, Phys. Rept. **287**, 447 (1997) [arXiv:hep-th/9602045].
- [30] V. S. Kaplunovsky, Nucl. Phys. B **307**, 145 (1988) [Erratum-ibid. B **382**, 436 (1992)] [arXiv:hep-th/9205068];
 L. J. Dixon, V. Kaplunovsky and J. Louis, Nucl. Phys. B **355**, 649 (1991).
- [31] K. R. Dienes, Nucl. Phys. B **429**, 533 (1994) [arXiv:hep-th/9402006];
 K. R. Dienes, M. Moshe and R. C. Myers, Phys. Rev. Lett. **74**, 4767 (1995) [arXiv:hep-th/9503055].
- [32] K. R. Dienes, Ph.D. thesis (Cornell University, May 1991), UMI-9131336.
- [33] J. Balog and M. P. Tuite, Nucl. Phys. B **319**, 387 (1989).
- [34] See, *e.g.*, K. R. Dienes and A. E. Faraggi, Phys. Rev. Lett. **75**, 2646 (1995) [arXiv:hep-th/9505018]; Nucl. Phys. B **457**, 409 (1995) [arXiv:hep-th/9505046];
 K. R. Dienes, A. E. Faraggi and J. March-Russell, Nucl. Phys. B **467**, 44 (1996) [arXiv:hep-th/9510223].
- [35] K. R. Dienes, M. Lennek, V. Wasnik *et al* (in progress).
- [36] K. R. Dienes, Nucl. Phys. B **611**, 146 (2001) [arXiv:hep-ph/0104274].